REGIONAL VARIATION OF PERIFOVEAL ACUITY, RETINAL THICKNESS AND RETINAL CONTOUR IN MYOPIA

A thesis presented to the graduate faculty of
New England College of Optometry in partial fulfillment
of the requirements for the degree of Master of Science

Stephanie X. Shao

April, 2013

©Stephanie X. Shao
All rights reserved

The author hereby grants New England College of Optometry permission to reproduce and to distribute publicly paper and electronic copies of the thesis document in whole or in part.

REGIONAL VARIATION OF PERIFOVEAL ACUITY, RETINAL

THICKNESS AND RETINAL CONTOUR IN MYOPIA

Stephanie X. Shao

This manuscript has been read and accepted by the
Thesis Committee in satisfaction of the
thesis requirement for the degree of Master of Science

4-26-13
Date

Nancy J. Coletta, O.D., Ph.D.
Graduate Faculty Advisor

Jane E. Gwiazda, Ph.D.
Thesis Committee Member

Elise N. Harb, O.D., M.S.
Thesis Committee Member

David Troilo, Ph.D.
Thesis Committee Member

5-16-13
Date

Nancy J. Coletta, O.D., Ph.D.
Director of Graduate Studies

New England College of Optometry

REGIONAL VARIATION OF PERIFOVEAL ACUITY, RETINAL THICKNESS AND RETINAL CONTOUR IN MYOPIA

Stephanie X. Shao

New England College of Optometry, 2013

Abstract

Purpose: Myopic eyes exhibit retinal thinning which is thought to be associated with expansion of the globe during myopia development. If retinal thinning is due to retinal stretching, then cone density, and subsequently acuity, is expected to be lowest in areas of the retina that exhibit the most thinning. The first aim was to examine the relationship between acuity and retinal thickness. The second aim was to measure retinal contour in four retinal meridians and to examine how it changes as a function of refractive error, with the hypothesis that regions which exhibit the greatest expansion should be associated with greater stretching, and thus retinal thinning.

Methods: Forty-six healthy, non-presbyopic (age 22-39 years) subjects were included, with refractive errors ranging from +0.75 D to -9.50 D and less than 1.50 D astigmatism. Retinal thickness was measured in the macular region using spectral-domain OCT and compared to retinal acuity measurements acquired by interferometry at corresponding retinal locations.

Retinal thickness was analyzed for the full thickness from the retinal pigment epithelium (RPE) to the inner limiting membrane (ILM), as well as for outer retinal layer thickness (from RPE to inner plexiform layer, or IPL) and for inner retinal layer thickness (from IPL to ILM). Axial length was measured centrally and peripherally out to 40 degrees eccentricity in the vertical and horizontal meridians with a Zeiss IOL Master biometry system, and retinal contour coordinates were derived from these measurements.

Results: Myopia was correlated with retinal thinning and decreased retinal acuity in all four retinal quadrants of the perifoveal region. Worse visual acuity was associated with thinning in the superior retinal meridian in particular, though this effect was not statistically significant ($p=0.086$ for full retinal thickness and $p=0.08$ for outer retinal layer thickness). Asymmetries in retinal contour were found, with low myopes exhibiting relatively steeper inferior retina at 20 deg ($p=0.005$) and 30 deg ($p=0.015$) eccentricities, and high myopes exhibiting relatively steeper temporal retinas at 20 deg ($p=0.004$) and 30 deg ($p<0.001$) eccentricities. In the nasal region, retinal thinning in the perifovea is associated with shallower retinal contour or greater expansion of the globe at 10 deg eccentricity ($p=0.049$).

Conclusions: Regional variations exist in myopic eye growth, resulting in local differences in retinal thickness, retinal contour, and acuity.

Acknowledgements

I would like to express my gratitude to Dr. Nancy Coletta for being an amazing mentor and friend. It has been a pleasure to have you as my guide through this process. Also to my family and friends for the support and encouragement.

This research project was funded by New England College of Optometry and the following NIH grants: T35 EY007149, R24 EY014817, and R01 EY012847.

Table of Contents

1. Introduction

1.1. Retinal Thickness and Myopia 1
1.2. Photoreceptor Density 5
1.3. Effects of Myopia on Visual Acuity 6
1.4. Theories of Myopic Eye Growth 8
1.5. Peripheral Refraction and Eye Shape 8
1.6. Current Study Aims 11

2. Methods

2.1. Subjects 13
2.2. Study Procedures 13
2.3. Data Analysis 19

3. Results: Retinal Thickness and Acuity

3.1. Biometric Characteristics of Subjects 24
3.2. Relationship between Retinal Thickness and Axial Length 25
3.3. Ratios of Retinal Layer Thickness vs. Axial Length 31
3.4. Retinal Acuity and Axial Length 34
3.5. Retinal Acuity and Retinal Thickness 37

4. Results: Retinal Contour and Retinal Thickness

4.1. Biometric Characteristics of Subjects 41
4.2. Retinal Contours 41
4.3. Retinal Contour by Linear Retinal Eccentricity 48
4.4. Comparison of Results to a Published Study 51
4.5. Retinal Depth and Axial Length 53
4.6. Retinal Thickness and Retinal Contour 57

5. Discussion

5.1. Retinal Thickness 64
5.2. Acuity and Retinal Thickness 65
5.3. Retinal Layers and Retinal Function in Myopia 69
5.4. Retinal Contours in Myopia 70
5.5. Summary and Conclusions 74

6. Bibliography 76

7. Appendix

7.1. Consent Form 83
7.2. Recruitment message 88
7.3. Questionnaire 89

List of Figures and Tables

Figures

1.1 Sample OCT B-scan and macular thickness map 3
1.2 Models of myopic eye growth 8
1.3 Retinal stretching and cone density in myopia 12

2.1 OCT retinal thickness scan segmentation 16
2.2 Acuity measurement locations in relation to OCT thickness map 18
2.3 Calculation of IOL Master corneal entry position 21
2.4 Calculation of IOL Master retinal position 22

3.1 Axial length and refractive error 24
3.2 Foveal full, inner and outer retinal thickness vs. axial length 25
3.3 Parafoveal full retinal thickness vs. axial length 26
3.4 Parafoveal inner retinal thickness vs. axial length 27
3.5 Parafoveal outer retinal thickness vs. axial length 27
3.6 Perifoveal full retinal thickness vs. axial length 28
3.7 Perifoveal inner retinal thickness vs. axial length 30
3.8 Perifoveal outer retinal thickness vs. axial length 30
3.9 Parafoveal inner/full thickness ratio vs. axial length 32
3.10 Parafoveal outer/full thickness ratio vs. axial length 32
3.11 Perifoveal inner/full thickness ratio vs. axial length 33
3.12 Perifoveal outer/full thickness ratio vs. axial length 33
3.13 Foveal acuity vs. axial length and refraction 35
3.14 Perifoveal acuity vs. axial length and refraction 36
3.15 Retinal acuity vs. perifoveal full retinal thickness 37
3.16 Retinal acuity vs. perifoveal inner retinal thickness 38
3.17 Retinal acuity vs. perifoveal outer retinal thickness 38
3.18 Retinal acuity vs. perifoveal inner/full retinal thickness ratio 40
3.19 Retinal acuity vs. perifoveal outer/full retinal thickness ratio 40

4.1 Retinal depth coordinates in the vertical plane 42
4.2 Retinal depth coordinates in the horizontal plane 43
4.3 Retinal depth by refractive group, in the vertical plane 45
4.4 Retinal depth by refractive group, in the horizontal plane 46
4.5 Linear retinal contour coordinates 50
4.6 Relative peripheral eye lengths 52
4.7 Depth coordinates at 30 deg vs. axial length and refractive error 55
4.8 Depth coordinates at 10 deg vs. axial length and refractive error 56
4.9 Perifoveal thickness in the vertical meridian, by refractive error group 58
4.10 Perifoveal thickness in the horizontal meridian, by refractive error group 59
4.11 Retinal depth at 10 deg eccentricity vs. retinal thickness 62
4.12 Retinal depth at 30 deg eccentricity vs. retinal thickness 63

5.1 Comparison of retinal acuity and acuity predicted from cone density 66

Table

1.1 Summary of OCT studies of macular thickness 4

Introduction

Myopia is a global public health problem that leads to visual impairment and ocular complications with associated economic and social consequences. Myopia is prevalent in about 25% of the United States population and up to 80% of Asian populations (Pan, Ramamurthy, & Saw, 2011). The rise of the prevalence of myopia worldwide is a concern because of the associated increased risk of potentially blinding ocular conditions. For example, excessive elongation of the globe that occurs with high myopia can lead to pathological changes in the fundus such as retinal breaks, retinal detachment, chorioretinal atrophy, lacquer cracks, lattice degeneration, choroidal neovascularization, and posterior staphyloma. Myopia is also associated with an increased risk of cataracts, optic disc abnormalities, and glaucoma (Saw, Gazzard, & Chan Shih-Yen, 2005). The ocular health complications of myopia present a significant economic burden. The National Health and Nutrition Examination Survey (NHANES) reported the annual direct health costs of myopia in the United States to be between $3.9-$7.2 billion dollars (Pan, Ramamurthy, & Saw, 2011).

1.1 Retinal Thickness and Myopia

It is well accepted that axial elongation of the eye's vitreous chamber occurs with myopia (Curtin, 1985). Axial expansion with myopia results in scleral, choroidal, and retinal thinning as these structures stretch to cover the increased surface area of the globe. Evidence of choroidal stretching can be seen in the presence of optic disc crescents in

myopic eyes, in which the choroid and retinal pigment epithelium pull away from the optic nerve margin. Choroidal thinning may also cause breaks in Bruch's membrane, which present as lacquer cracks. Myopic eyes are also more prone to such pathologies as posterior staphyloma, posterior vitreous detachments, and retinal detachments as a result of retinal thinning (Curtin, 1985).

Recent studies have used optical coherence tomography (OCT) to investigate macular retinal thickness in myopes. OCT is an in-vivo imaging technique that utilizes coherent light to obtain high-resolution, cross-sectional images of the ocular structures. It allows retinal layers to be visualized and thickness measurements to be obtained for various retinal regions. Figure 1.1 (upper panel) shows a 6-mm long false-color retinal thickness section (B-scan) taken through the macula at a single orientation, in this case, vertically. The upper part of the figure is the vitreous side and the lower part of the figure is the choroidal side. The dip in the center of the scan indicates the foveal pit. Different colors in the figure represent tissue layers with different refractive indices. OCT scans of the macular region are typically divided into three concentric regions: the fovea is defined as the central 1 mm region, parafovea as the annular region with inner diameter of 1 mm and outer diameter of 3 mm, and perifovea as the annular region with inner diameter of 3 mm and outer diameter of 6 mm (Figure 1.1, upper). Retinal thickness in the parafoveal and perifoveal rings is further subdivided into nasal, temporal, superior and inferior quadrants, with the averaged retinal thickness, in microns, displayed in each region of the thickness map (Figure 1.1, lower).

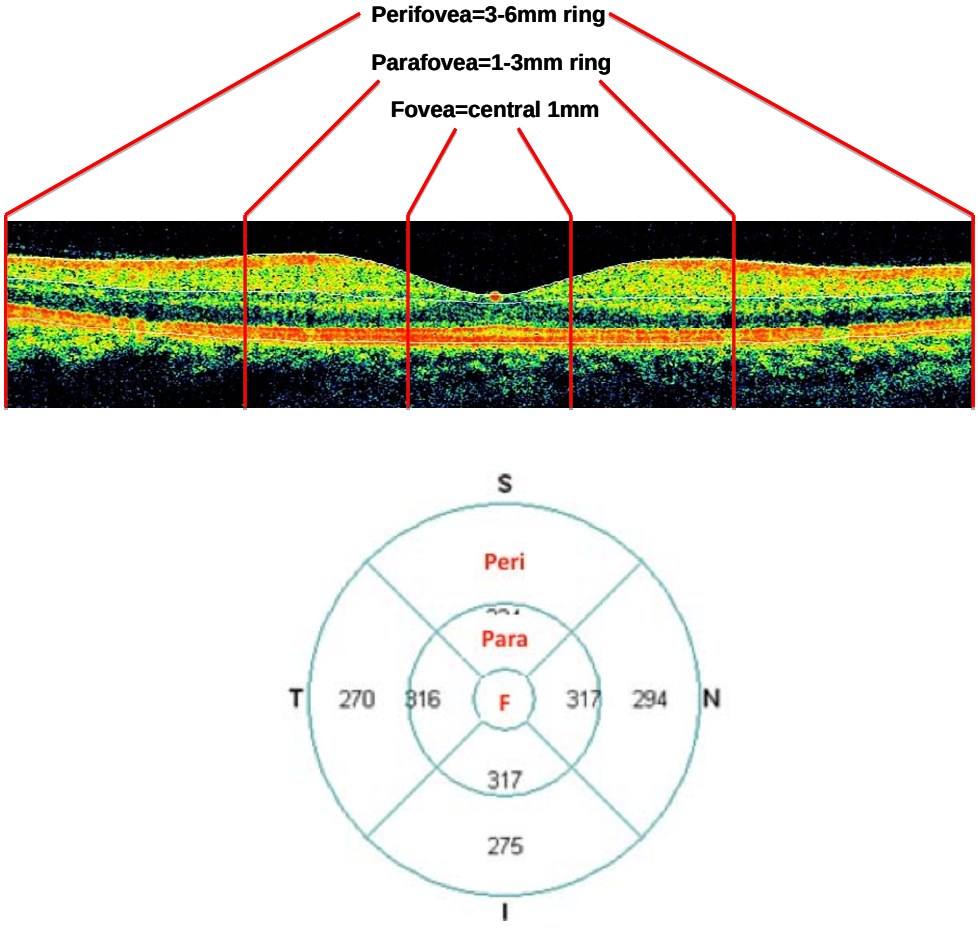


Fig 1.1. *Upper panel:* Sample 6-mm long OCT B-scan through the fovea. Regions show the central 1 mm, parafoveal ring from 1-3 mm eccentricity and perifoveal ring from 3-6mm eccentricity. *Lower panel:* Sample OCT macular thickness map segmented into the central 1 mm, or fovea (F), parafoveal (Para), and perifoveal (Peri) rings; the rings are subdivided into superior, inferior, nasal, and temporal quadrants.

Study	Fovea (central 1mm)	Parafovea (1-3mm ring)	Perifovea (3-6mm ring)
Lim et al. (2005)	Thickening	Thinning	No sig. diff.
Luo et al. (2006)	Thickening	Thinning N and T	Thinning
Lam et al. (2007)	Thickening	No sig. diff.	Thinning
Wu et al. (2008)	Thickening	Thinning	Thinning
Xie et al. (2009)	No sig. diff.	Thinning except N	Thinning except S
Song et al. (2010)	No sig. diff.	No sig. diff.	Thinning
Sato, Fukui & Ohta (2010)	Thickening	Thinning I and N	Thinning T
Harb et al. (2012)	Thickening	Thinning	Thinning

Table 1.1. Summary of OCT studies of macular thickness changes with myopia. All studies except Harb (2012) examined perifoveal thickness in the 3-6 mm wide ring; while the Harb study examined perifoveal thickness in the 3-5 mm wide ring.

Results of macular thickness OCT studies in myopia, published since 2005, are summarized in Table 1.1. Most studies find that the perifoveal region is thinned in myopic eyes when compared to emmetropic eyes. The pattern of results in the parafoveal ring is not as consistent, and results tend to vary among the four quadrants, but generally myopes tend to exhibit thinning of the retina in the parafoveal region. Unlike thinning observed in the parafoveal and perifoveal rings, myopes tend to have greater retinal thickness in the central 1 mm region compared to emmetropes. This is a somewhat surprising result, but it is theorized to be related to the shape of the foveal pit, such that biomechanical tension in the lateral direction that results during eye growth may result in movement of the floor of the foveal pit toward the vitreous (Wu et al., 2008). On the

other hand, other factors in the development of the foveal pit potentially could be different in myopic eyes than in emmetropic eyes. Analysis of macular thickness in very young eyes would be required to determine whether foveal thickening is a result of retinal stretching in myopic eyes or whether it might even be present in eyes destined to become myopic, before the expansion of the globe.

There have been few studies examining the thickness of retinal layers in myopia but one study that used time-domain OCT reported that peripheral retinal thinning in myopia was mainly due to thinning of the middle and inner retinal layers and not to changes in thickness of the photoreceptor layer (Wolsley et al., 2008). Advances in OCT technology, in particular, the introduction of spectral-domain OCT to clinical research, have provided a way to examine alterations of retinal layer thickness in myopia with more accuracy. The variation in inner and outer retinal layer thickness, divided at the inner plexiform layer, has not been described in myopic adults, nor has it been related specifically to acuity, so this analysis was performed in the current study with spectral-domain OCT.

1.2 Photoreceptor Density

The number of cone photoreceptors present in the human retina reaches final adult numbers by 11-15 months of age (Hendrickson, 1992), so the eye growth associated with developing myopia in childhood through early adulthood should effectively result in greater cone spacing as the retina is stretched. Kitaguchi et al. (2007) and Chui et al.

(2008) used adaptive-optics imaging techniques to compare cone density in myopes and emmetropes. In both studies, cone packing density was found to be significantly lower in highly myopic eyes compared to emmetropic eyes, evidence for retinal stretching as a result of myopic eye growth. This result implies that a fixed number of cones is distributed over a larger retinal surface in the myopic eye, thereby resulting in a decrease in cone density. In the Chui et al. (2008) study, the inferior retinal quadrant was found to have the lowest cone density compared to other retinal regions in all subject groups. In comparison to emmetropes, myopes showed the greatest decrease in cone density in the temporal and inferior retina at a retinal eccentricity of 2.0 mm, which is in the perifoveal region.

1.3 Effects of myopia on visual acuity

Visual acuity is closely associated with cone spacing, as the fall-off in acuity over the peripheral visual field closely parallels the increase in cone spacing, or decrease in cone density, with retinal eccentricity (Wertheim, 1980; Williams & Coletta, 1987). Coletta and Watson (2006) and Atchison et al. (2006) used interferometry to measure the visual acuities of myopes and emmetropes. This technique eliminates any effects of optical quality differences among subjects, allowing a direct comparison of retinal acuities between myopes and emmetropes. In the Coletta and Watson study, acuity was tested using grating acuity stimuli formed directly on the retina at the fovea, 4° and 10° eccentricities. It was found that myopes had decreased retinal acuity compared to emmetropes both at the fovea and parafoveal regions. Acuity data from the Coletta and

Watson study supports a model of eye growth in myopia in which mainly the posterior pole expands (Strang et al., 1998).

The acuity loss in myopes can be attributed to reduced sampling due to greater cone spacing as a result of retinal stretching. Chui et al. (2008) compared parafoveal cone spacing measured with adaptive optics to parafoveal retinal acuity gathered in the Coletta and Watson study. The acuities predicted from cone spacing were not an exact match to the retinal acuities; however acuity and cone spacing data fell off with increasing myopia at very similar slopes, even though these studies were not performed on the same subjects.

Myopes therefore exhibit losses in acuity in the parafoveal and perifoveal regions that mirror the losses of cone density, and these retinal regions coincide with regions that exhibit retinal thinning in the OCT studies. The coarser grain in myopia has been attributed to retinal stretching, consistent with expansion of mainly the posterior part of the eye (Chui et al., 2005; Coletta & Watson, 2006). Reductions in acuity in myopia may be most evident in retinal areas with the most evidence for expansion of the eye. Stretching of the globe may not be uniform and may thus affect certain regions or meridians of the visual field more than others. Some psychophysical studies suggest that the functional effects of retinal stretching are more apparent in the parafovea and near periphery than in the fovea (Choi *et al.*, 2003; Vera-Diaz *et al.*, 2005). Expansion of the globe, with subsequent mechanical stretching of the retina, has been offered as an explanation for increased meridional effects in spatial vision that are observed in the periphery of myopic subjects (Vera-Diaz et al., 2005).

1.4 Theories of Myopic Eye Growth

Three models of myopic eye growth have been suggested by Strang et al. (1998). The global expansion model (Fig. 1.2a) involves uniform expansion across the globe, resulting in vitreous chamber elongation. The equatorial expansion model (Fig. 1.2b) describes elongation axially, only at the equatorial region of the globe. Finally, the posterior pole model (Fig. 1.2c) describes growth selectively at the posterior pole in a radial manner. Each model predicts a peripheral refraction of relative hyperopia in the periphery of myopic eyes, with the posterior pole model predicting the greatest degree of relative peripheral hyperopia and the global expansion model predicting the least.

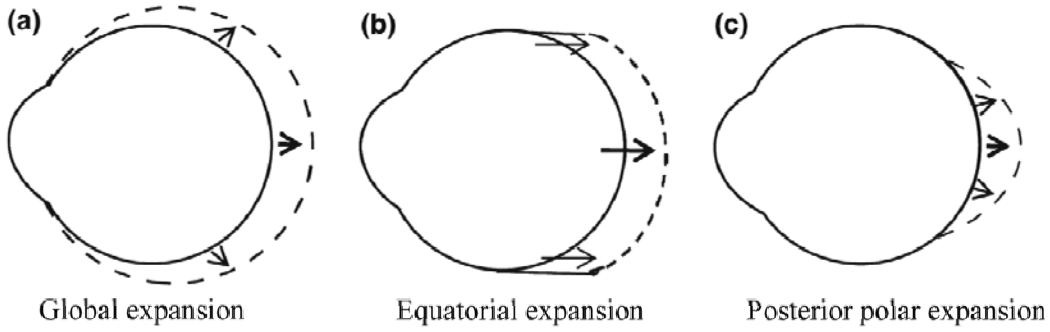


Fig. 1.2. Models of myopic eye growth as proposed by Strang et al. (1998).

1.5 Peripheral Refraction and Eye Shape

Previous studies have investigated the role of peripheral refraction in myopia development. Light from a distant off-axis point may converge either at the retinal

surface, in front of, or behind the retinal surface. Convergence in front of the retinal surface would result in peripheral myopic defocus. Conversely, convergence behind the retinal surface would result in peripheral hyperopic defocus. Wallman and Winawer (2004) suggested that peripheral defocus could drive development of central refractive error because of the presence of more neurons in the periphery in comparison to the fovea.

Retinal shape has been deduced indirectly using optical methods, including peripheral refraction and partial coherence interferometry. Evidence has shown that myopic growth of the eye occurs primarily axially, resulting in a relatively prolate, or less oblate, retinal contour compared to emmetropic or hyperopic eyes. Logan et al. (2004) used peripheral refraction, corneal curvature, and axial biometry data to derive retinal shape in a study investigating differences in retinal contour in adult anisomyopes. Comparing eyes within individual subjects, it was found that the more myopic eyes exhibited greater elongation and more prolate shape relative to the less myopic eyes.

Mutti et al. (2000) assessed ocular shape in children by measuring peripheral refraction and found that myopic eyes had greater relative hyperopia in the periphery, indicating a prolate retinal contour. Low amounts of relative peripheral myopia were measured in emmetropic children, indicating a near spherical or oblate eye shape. Higher amounts of relative peripheral myopia were measured in hyperopic children, indicating an oblate retinal contour. Recent studies in children have found that relative peripheral refraction is not predictive of myopia development (Mutti et al., 2011; Sng et al., 2011). These studies found no differences in relative peripheral refraction between emmetropes who become myopic and those who remain emmetropic.

Besides peripheral refraction, ocular shape can also be derived indirectly from peripheral eye length measurements using partial coherence interferometry. Partial coherence interferometry compares the optical path lengths of two light beams, one reflected off the corneal surface and the other off the retina, thereby giving the cornea to retina eye length. Atchison and Charman (2011) calculated peripheral eye lengths of schematic eyes and confirmed the validity of partial coherence interferometry in estimating retinal contours. Schmid (2003) developed his own partial coherence interferometer to measure cornea to retina lengths centrally and up to 20^{o} peripherally in children. Retinal steepness was measured by subtracting the central length from the peripheral length. Using this method, the peripheral retina of myopic eyes was described to be steeper compared to emmetropic and hyperopic eyes. Mallen and Kashyap (2007) devised an external attachment for the IOLMaster, a commercially available device utilizing partial coherence interferometry, to measure peripheral eye lengths out to 40^{o}. Retinal contour was described by plotting the measured lengths at each eccentricity, but results were only reported for two subjects.

Eye shape has also been investigated using direct imaging techniques, including X-ray, computed tomography (CT), and magnetic resonance imaging (MRI). There is good agreement in characterization of myopic eye growth between imaging techniques. In an early study by Deller et al. (1947) using X-ray techniques, myopic eyes were reported to have greater axial lengths than transverse (height and width) lengths. Similar findings were reported by Song et al. (2007) in a study of 406 eyes using CT imaging, demonstrating greater increases in axial length than height and width in myopes. Atchison et al. (2004) compared dimensions of myopic and emmetropic eyes using MRI.

Myopic eyes were found to be larger in length, height, and width in a ratio of 3:2:1, with the most significant growth observed in axial length.

1.6 Current Study Aims

The first aim of the current study was to examine the relationship between acuity and retinal thickness in the same group of subjects. Previous studies have measured retinal thickness and acuity in separate subjects, so data on retinal thickness and visual acuity obtained in the same eyes in the same retinal locations would be valuable in understanding the relationships between these parameters. If thinning is due to retinal stretching, then it is expected that cone density would be lowest in areas of the retina that exhibit the most thinning (Fig. 1.3).

Retinal areas with lower cone density should show correspondingly greater relative losses of visual acuity. Thus, areas that exhibit the greatest retinal thinning should correlate with areas of greatest relative acuity loss in myopes. Focus was paid on the perifoveal region since this is the area that has demonstrated the most consistent effects of retinal thinning in prior OCT studies. In contrast, there was not expected to be a good correlation between foveal acuity and foveal retinal thickness, since the fovea seems to be subject to different biomechanical effects from myopic eye growth, showing thickening with increasing myopia. Retinal thickness was compared in the four retinal quadrants of the perifoveal region. Since myopic eyes may have different optical characteristics than emmetropic eyes, acuity was measured in the same perifoveal retinal

areas in four meridians, using a technique that by-passes the eye's optical effects and thus provided a measure of acuity at the retinal, or neural level.

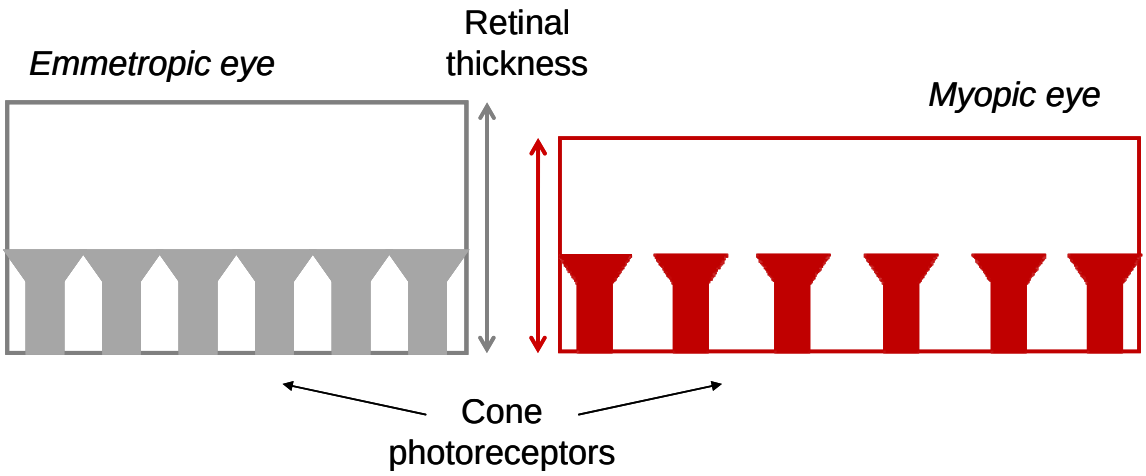


Fig. 1.3 Retinal thinning in the myopic eye. A fixed number of cones distributed over a larger retinal surface area in the myopic eye results in decreased cone density (increased cone spacing) compared to an emmetropic eye.

A second aim of the current study was to measure retinal contour in four retinal meridians, and to examine how it changes as a function of refractive error. Eye growth during myopia development may affect some regions of the globe more than others. For example, nasal-temporal asymmetry in eye shape (Ehsaei et al., 2013, Logan et al., 2004) might mean that the nasal retina undergoes greater expansion than the temporal meridian in myopic eyes. Meridians of the eye that exhibit the greatest expansion would be expected to also exhibit the greatest retinal thinning in OCT measures. This is because greater expansion should be associated with greater stretching and thus retinal thinning.

2. Methods

2.1 Subjects

Subjects were recruited from the New England College of Optometry faculty, staff, and students via an e-mail message. The study protocol was approved by the New England College of Optometry (NECO) Institutional Review Board (see Appendix I). All measurements were performed only on the left eye in all subjects due to the logistical set up of the devices used in data collection. Subjects were required to have best corrected visual acuity of at least 20/30 in the left eye after a subjective refinement of the refraction. Subjects had adequate hearing, language skills, and mental ability to understand the consent process and the instructions during the experiment. Only subjects with refractive error ranging from low hyperopia (≤ +2.00D) to high myopia (up to -12.00D) with central astigmatism ≤1.50D were included in the study. Exclusion criteria included the following: visual acuity not correctable to at least 20/30 in the left eye; cataract or other media opacity; fixational instability (e.g., nystagmus) or restricted movement of either eye; history of ocular pathology, eye injury or surgery, or orthokeratology; any present ocular medications; age under 18 years. Forty-six subjects were recruited for the study; a subset of thirty-six subjects was available for interferometric acuity measurements in all four retinal meridians.

2.2 Study Procedures

Data measurements were collected over two sessions for each subject. In the first session, entrance visual acuity was first assessed monocularly in the left eye for inclusion

or exclusion. Visual acuity was measured with the subject's refractive correction (spectacles or contact lenses) at a distance of 10 feet using a 100% contrast Bailey-Lovie logMAR letter chart. The refractive correction was subjectively modified using loose trial lenses to obtain the best corrected visual acuity.

Central autorefraction was then measured with a Wavefront Sciences Complete Ophthalmic Analysis System (COAS), which uses the Shack-Hartmann wavefront sensing technique. Subjects were seated at a chinrest and forehead restraint with the room lights dim to maximize pupil size. Subjects were asked to fixate a central, non-accommodative target and five measurements of the refraction were made. The Zernike 2^{nd} order terms along with the 4^{th} order spherical aberration term (Seidel sphere) were averaged from the five readings and converted to a sphere, cylinder and axis of refraction.

Central axial length and peripheral eye length were then measured with a Zeiss Meditec IOL Master biometry system. This device is non-contact and uses a low-power laser interference technique, partial coherence interferometry, to measure axial length. The IOL Master measures the distance from the corneal tear film to the retinal pigment epithelium; however, the reading is adjusted automatically to represent the distance from the tear film to the inner limiting membrane in order to make the readings comparable to ultrasound axial length measures (Zeiss IOL Master User's Manual, 2004). The IOL Master technique has been shown to be more accurate and repeatable than ultrasound (Lam et al., 2001; Sheng et al., 2004). The device also uses optical pachometry to measure the anterior chamber depth of the eye. Measurements of the central axial length and the anterior chamber depth were made on the left eye, with five readings for each measurement. Two measurements were then taken at each of following peripheral

locations: from 10 to 40 degrees eccentricity in 10 degree increments superiorly, inferiorly, nasally and temporally. Fixation for off-axis positions in the IOL Master were controlled with fixation marks on a printed card mounted to the front of the IOL Master. The fixation marks were black dots surrounded by black numbers, indicating the eccentricity in degrees, printed on a white card. The fixation marks subtended 1.1 deg and the numbers subtended 4 deg. The subject was instructed by the examiner to look at the corresponding fixation mark at the different degree locations. The subject did not wear refractive correction during these measurements and room illumination was kept dim so that the pupil diameter was large. Most subjects were able to be measured out to 30 degrees eccentricity. About half of the subjects could be measured out to 40 degrees. For subjects who could not be measured at 40 degrees, attempts were made to measure their peripheral eye lengths at 35 degrees.

Central corneal power was measured with a Zeiss Humphrey Atlas 995 corneal topographer, taking four readings. The averaged central corneal power from the topographer, along with the averaged anterior chamber and central axial length measurements from the IOL Master, were used to construct a three-surface model eye for each subject. The model eyes were used to convert acuity in cyc/deg to retinal acuity in cyc/mm in order to make acuity equivalent across eye size (Coletta and Watson, 2006).

Retinal thickness was then measured with an Optovue RTVue Spectral Domain OCT. Retinal thickness in the macular region was measured with the MM6 scan pattern included in the software program of the RTVue. The MM6 scan pattern consists of twelve 6-mm long scans that rotate through the fovea at 15° intervals. Three MM6 scans were performed for each subject. These measurements provided the full retinal thickness,

taken from the retinal pigment epithelium (RPE) to the inner limiting membrane (ILM), as well as the thickness of the outer and inner retinal layers. An example of how the software segments the retinal thickness scan is shown in Figure 2.1. A sample OCT B-scan through the fovea is shown. The vitreous is in the upper part of the figure, while the choroid is in the lower part of the figure. The OCT software segmented the image in three places: at the inner limiting membrane (ILM; upper white line); at the inner plexiform layer (IPL, middle white line) and at the retinal pigment epithelium (RPE, lower white line). Inner retinal thickness is measured from the ILM to the IPL, and outer retinal thickness is measured from the IPL to the RPE.

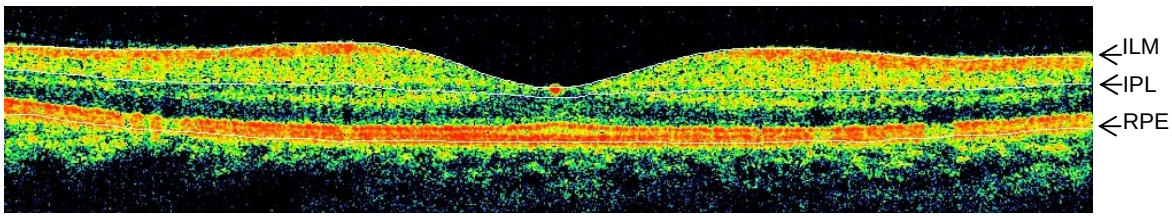


Fig. 2.1. OCT retinal thickness scan segmented into inner and outer retina at the inner plexiform layer (IPL)

Each MM6 measurement was checked for errors in placement of the segmentation lines in each of the twelve B-scans, and if segmentation lines needed adjustment (such as not following the foveal pit exactly or not following the ILM or RPE all the way to the edge of the scan) the lines were manually redrawn in such cases. After manual correction of the segmentation lines, the thickness map data were re-processed. Macular thickness was recorded by retinal regions according to the classification shown in Figure 1.1. Retinal thickness was analyzed for the fovea (central 1mm), parafovea (1-3mm diameter

ring), and perifovea (3-6mm diameter ring), and for the superior, inferior, nasal, and temporal quadrants.

In the second visit, visual acuity was measured with laser interferometry. Visual acuity of the left eye was measured with a custom-built optical system that images laser interference fringes directly on the retina (Coletta and Watson, 2006). Subjects were aligned with the optical system using a chin rest and head restraint. The contrast of interference fringes is unaffected by uncorrected refractive error, but the field stop in the interferometer, which defines the edge of the grating patch, can appear doubled with an uncorrected refractive error. For refractive errors less than 4.00 D of myopia or hyperopia, the field stop position was adjusted for each subject in order to maintain a single appearance of the field stop. Subjects with refractive errors greater than 4.00 D of myopia or hyperopia were corrected with either their habitual soft contact lenses or with their habitual spectacles; trial lenses were used if their habitual spectacles were tinted.

Testing was performed in the fovea and at 7 degrees eccentricity in the temporal, nasal, superior and inferior retina. These regions corresponded to the perifoveal OCT retinal thickness measurements, as shown in Figure 2.2. The 543 nm laser fringes were presented in a 2-degree diameter patch surrounded by a luminance-matched 8-degree annulus. The retinal illumination level of the interference fringe display was adjusted to 100 trolands with neutral density filters. Subjects were instructed to fixate the center of the grating patch for the foveal acuity measurements. For the peripheral acuity measurements, a small dim red blinking LED was used to guide fixation. The LED fixation light was positioned at the proper location with a magnet.

Acuity was determined using a two-alternative forced-choice orientation discrimination task. A tone signified when a fringe grating stimulus was presented. During the tone, a 100% contrast grating was presented for 200 msec, either vertical or horizontal in orientation, and the subject's task was to indicate the fringe orientation through the use of a joystick controller. Grating stimuli were presented for 20 trials at each of about 8 randomly interleaved spatial frequencies. The responses were used to construct a psychometric function, plotting the percent correct vs. spatial frequency. A Weibull function was fit to the acuity data using Kaleidagraph software and the acuity limit was defined as the spatial frequency corresponding to the 75% correct level.

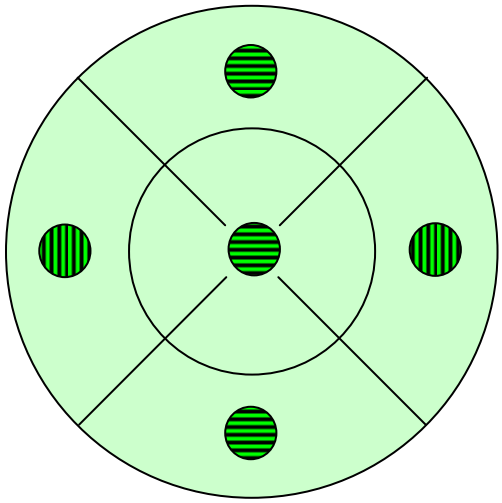


Fig 2.2. OCT retinal thickness rings (light green) with interferometric acuity fringe patches (darker green stripe patterns) superimposed at the fovea and at the perifoveal quadrants, indicating the retinal regions in which acuity was measured.

2.3 Data Analysis

2.3.1 OCT data analysis

Three macular MM6 scans for each subject were exported from the Optovue OCT machine using RTVue software. The exported data included measurements of retinal thickness and volume at the fovea, parafovea, and perifovea, each region divided into superior and inferior hemispheres, and four retinal quadrants. It included measurements for the full retinal layers, as well as inner retinal layers. Outer retinal layer measurements were calculated by subtracting the inner retina measurements from the full retina measurements. Averages of three macular scans were done for each subject. Measurements of minimum foveal thickness were manually recorded from the OCT machine. Since eye size can affect the region covered by an OCT scan, full retinal thickness data were adjusted for axial length magnification (Coletta, 2011, ARVO abstract). The effect of this adjustment was examined for the central 1 mm and perifoveal quadrants since the derived thickness in these macular regions is most susceptible to variation in OCT scan length.

2.3.2 IOL Master data analysis

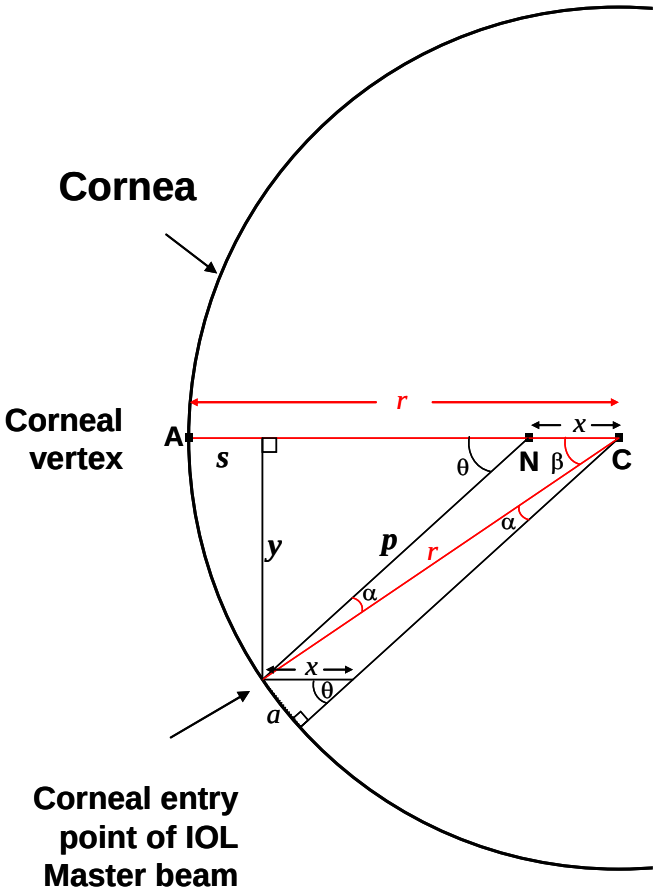
Data from the IOL Master was averaged for the central axial length and for each peripheral location. When data from different eye sizes are compared in angular units of eccentricity, the eye size affects the retinal position of the peripheral measurement. In order to compare data at the same retinal locations, rather than just at the same angular positions, data from the peripheral IOL Master measurements were converted to retinal

contour coordinates by a computing scheme that is based on first calculating the corneal entry position of the beam and then using trigonometry to calculate the position of the beam at the retina.

The total distance measured by the IOL Master is assumed to be the distance from the corneal entrance position to the retina, assuming the beam travels through the eye's nodal point (Atchison and Charman, 2011). The nodal point represents the position in the eye for which a beam would traverse undeviated at the angle of eccentricity (aiming angle). The nodal position of each subject's eye was estimated from construction of a three-surface model eye for each subject. Details of the three-surface eye computation are provided in Coletta and Watson, 2006. The three-surface model eye used the central corneal power from corneal topography, the central axial length from the IOL Master measurement, and the subject's refraction. The eye then provides the locations of the nodal points relative to the anterior corneal surface. For the current study, a single nodal point was estimated as being positioned halfway between N and N' in the three-surface model.

The corneal entry position of the beam is determined by the scheme outlined in Fig. 2.3. The diagram illustrates the geometry used to calculate the corneal entry position of the IOL Master beam from the corneal radius of curvature (r) which is the distance from the anterior vertex of the cornea (point A in Fig. 2.3) to the center of curvature of the cornea (point C in Fig. 2.3), the nodal point position (N) from the anterior vertex, and the angle of eccentricity (θ). Using geometry as shown in Fig. 2.3, distance x and angle θ are used to estimate distance a on the cornea, then distance a and the radius are used to calculate angle α; angle α is used to calculate angle β which in turn in used to calculate

distance *y*, the chord coordinate of the corneal entry position of the IOL Master beam. The sag, or depth coordinate, (*s*) of the corneal entry position is then obtained from *y* and *r*. Together the *s* and *y* coordinates give the corneal entry position which is then used to determine distance *p* from that entry position to the nodal point N. The distance *p* is the distance traveled by the IOL Master beam from the cornea to the nodal point.



Calculate corneal entry position of IOL Master beam

Assumptions:
Spherical Cornea
Single Nodal point of eye (halfway between N, N')

Know:
Corneal radius of curvature (distance *r*, shown red)
Distance from vertex to eye's nodal point (A to N)
from 3-surface model eye data
Angular eccentricity of measurement (theta)

Scheme calculates:
Distance x
Distance a
Angle alpha
Angle beta
Distance y (eccentricity coordinate from vertex)
Distance s (sag or depth coordinate from vertex)
Distance p (distance from corneal entry to N)

Together the s and y coordinates
give the position on the cornea
where IOL Master beam entered,
and distance p is the path of the IOL Master beam
from cornea to N

Fig. 2.3 Calculation scheme for determining the corneal entrance position of the IOL Master beam. Details in text.

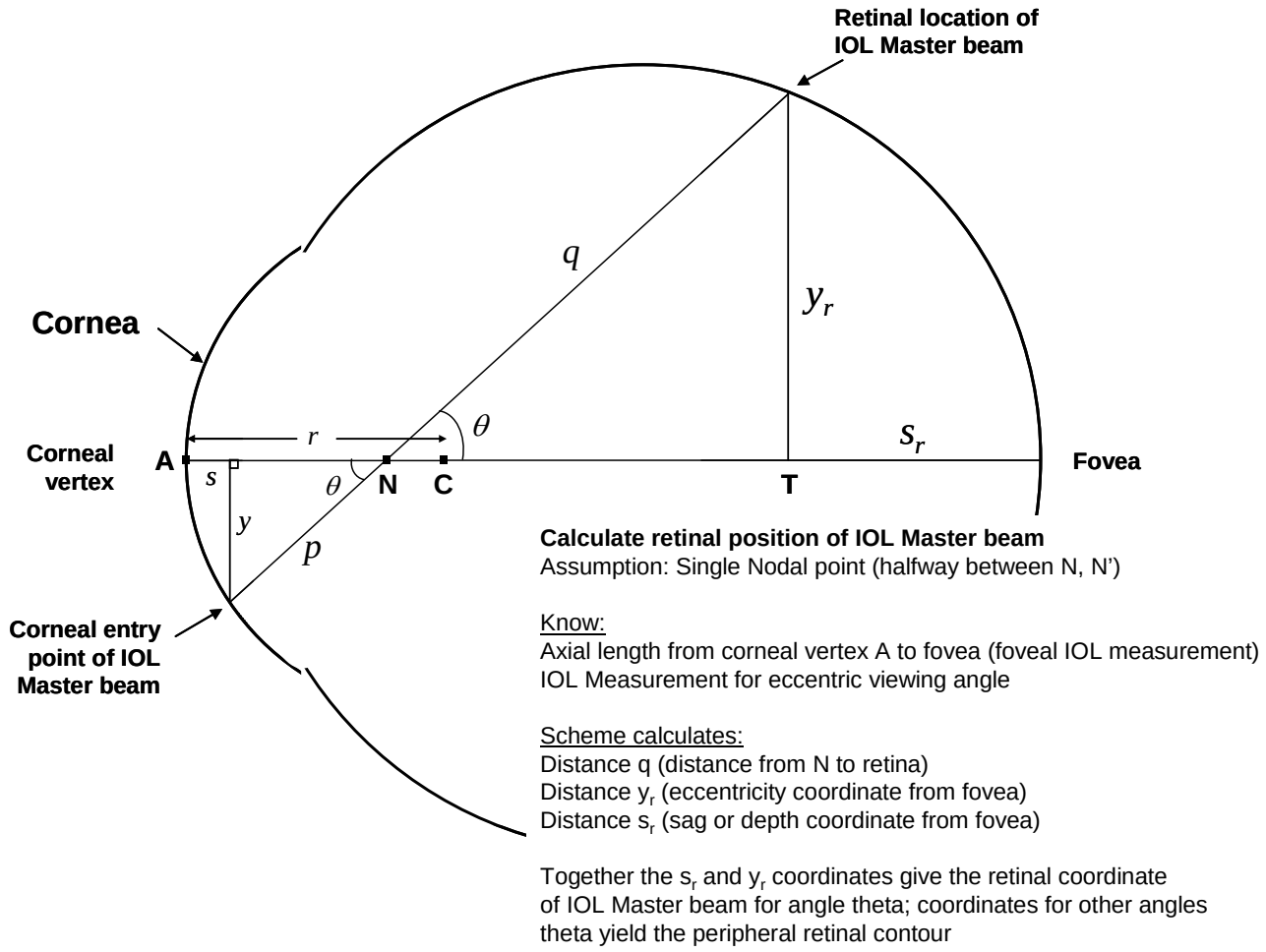


Fig. 2.4. Calculation scheme for determining the retinal coordinate of the IOL Master beam. Details in text.

Figure 2.4 shows how distance *p* is then used to calculate the retinal coordinate of the IOL Master beam. The total IOL peripheral measurement is the distance *p* plus *q*, so the distance *q* is determined by simply subtracting distance *p* from the peripheral IOL Master measurement. From distance *q* and the sine of angle θ, the retinal chord

coordinate, y_r, is calculated. The distance from N to point T in the diagram is determined from q and the cosine of angle θ. The distance from A to T is subtracted from the central axial length measurement, thus providing the sag or depth coordinate, s_r, of the retina.

2.3.3 Statistical analysis

Regression analysis was performed to investigate the relationship between retinal thickness in each retinal quadrant and axial length. Separate analyses were performed for full, inner, and outer retinal thickness. Regression analysis was also done correlating retinal thickness and acuity measurements at each retinal quadrant.

Retinal thickness and retinal contour measurements were also analyzed by refractive error. Subjects were divided into four refractive groups by spherical equivalent refractive error. The emmetropic group included subjects with refractive error between +0.75 D and -0.75 D. The low myopic group included subjects with refractions ranging from -1.00 D to -3.00 D. Moderate myopes included subjects with refractive error ranging from -3.00 D to -6.00 D, and the high myope group included subjects with refractive errors of more than -6.00 D of myopia. The retinal thickness and calculated retinal depth and eccentricity coordinates were averaged for subjects in each group, and data were compared for each refractive group in the vertical and horizontal meridians. Regression analysis was also performed to investigate the relationship between retinal contour, axial length, and OCT retinal thickness.

3. Results: Retinal Thickness and Acuity

3.1 Biometric characteristics of the subjects

Refractive errors of the 36 subjects for which acuity measurements were available ranged from +0.25 D to -9.50 D with less than 1.50 D astigmatism; average refraction was -3.32 D ± 2.76 s.d. Age ranged from 22 to 31 years with an average of 24.45 years ± 1.77 s.d. Central corneal power ranged from 40.6 to 47.3 D with an average of 44.3 D ± 1.52 s.d. Anterior chamber depth ranged from 2.17 to 4.19 mm with an average of 3.22 mm ± 0.67 s.d. Axial lengths ranged from 22.5 to 27.3 mm with an average of 24.49 mm ± 1.26 s.d. Axial length was strongly correlated with refractive error ($p<0.001$; $r^2=0.646$), in which an increase in myopic refractive error was associated with an increase in axial length (Fig. 3.1). Given this close correlation, further data analysis is presented based on axial length, although similar results were found with refractive error.

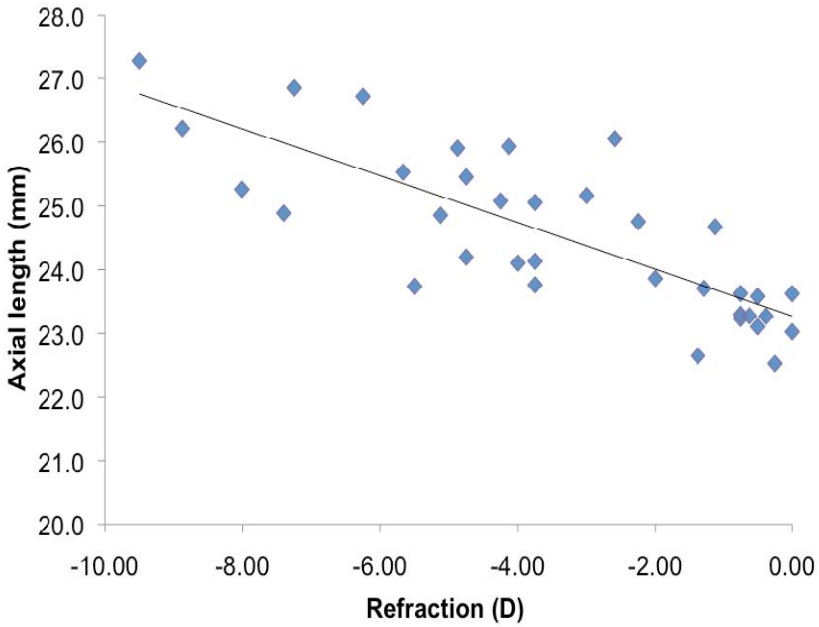


Fig. 3.1. Axial length in mm vs. refractive error in Diopters.

3.2 Relationship between retinal thickness and axial length

Full retinal thickness at the fovea, or central 1 mm, increased with axial length (Fig. 3.8), approaching statistical significance (p=0.061). Although the inner retinal layers are not anatomically present at the foveal pit (see Fig. 2.1), the OCT software segmented the central 1 mm of the macular scan into outer and inner retinal layers, indicating about 50-70 microns of inner retinal layer thickness in the central 1 mm region. The inner retinal thickness increased significantly with axial length (p=0.027), while the outer retinal thickness did not show a significant change with axial length.

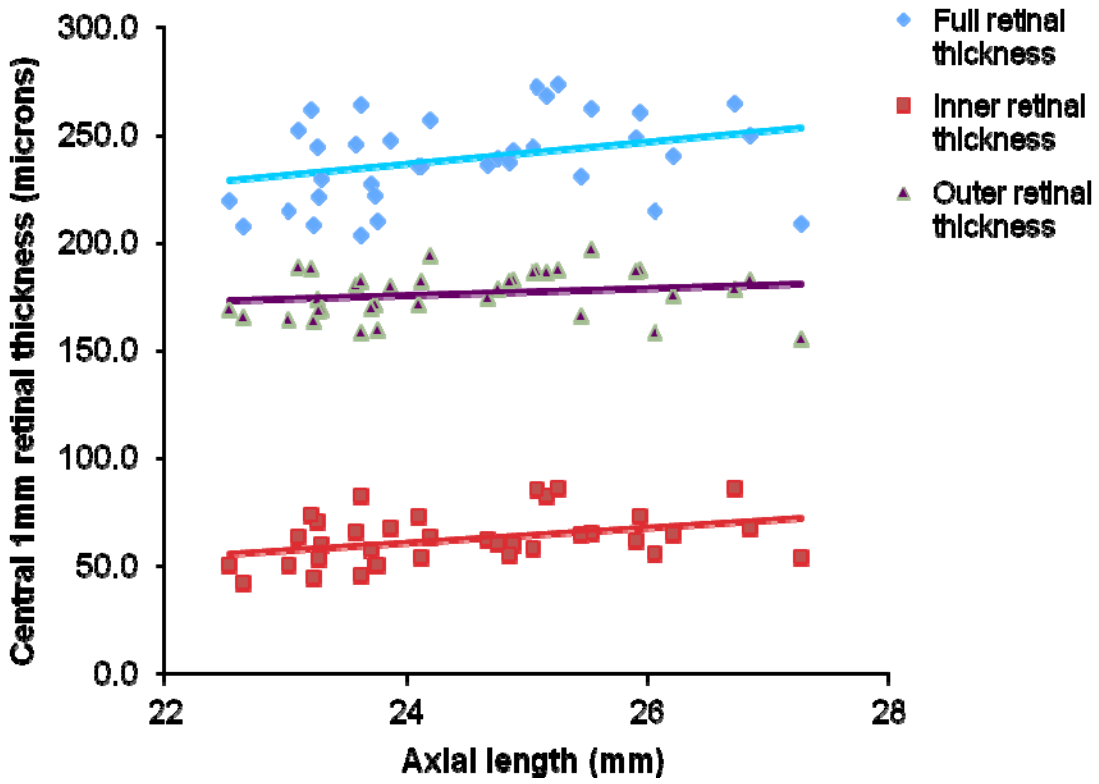


Fig. 3.2. Foveal (central 1 mm) full, inner, and outer retinal thickness changes with axial length.

In the parafoveal region (1-3 mm ring), full retinal thickness was greatest in the inferior quadrant and thinnest in the temporal quadrant. Retinal thickness did not vary significantly with axial length in any retinal quadrant. No statistically significant changes in full retinal thickness (Fig. 3.2), inner retinal layer thickness (Fig. 3.3), or outer retinal layer thickness (Fig. 3.4) were observed against axial length in any parafoveal quadrant. In the temporal parafoveal quadrant, the outer retinal layers thinned with increasing axial length, approaching statistical significance ($p=0.074$; $r^2=0.030$).

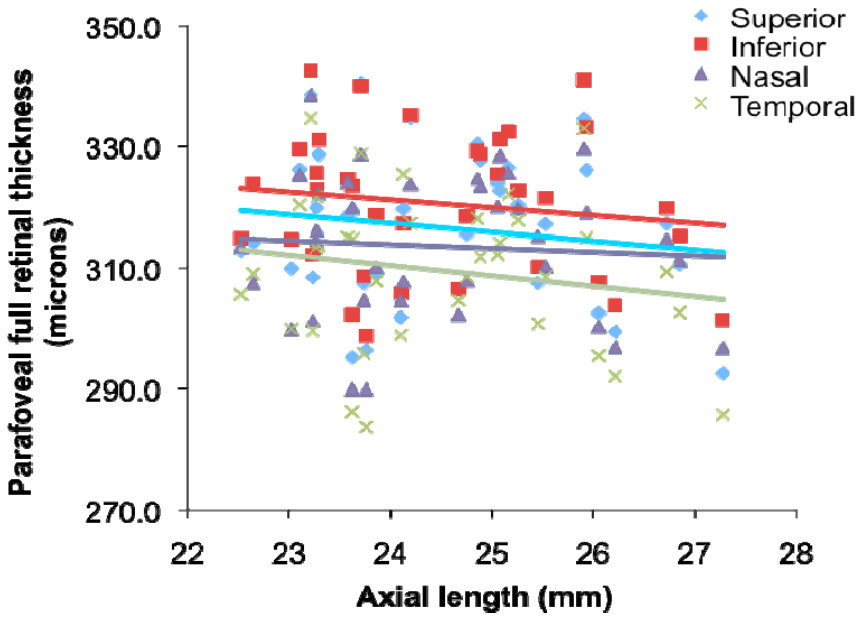


Fig. 3.3. Parafoveal (1-3 mm) full retinal thickness and axial length by retinal quadrant.

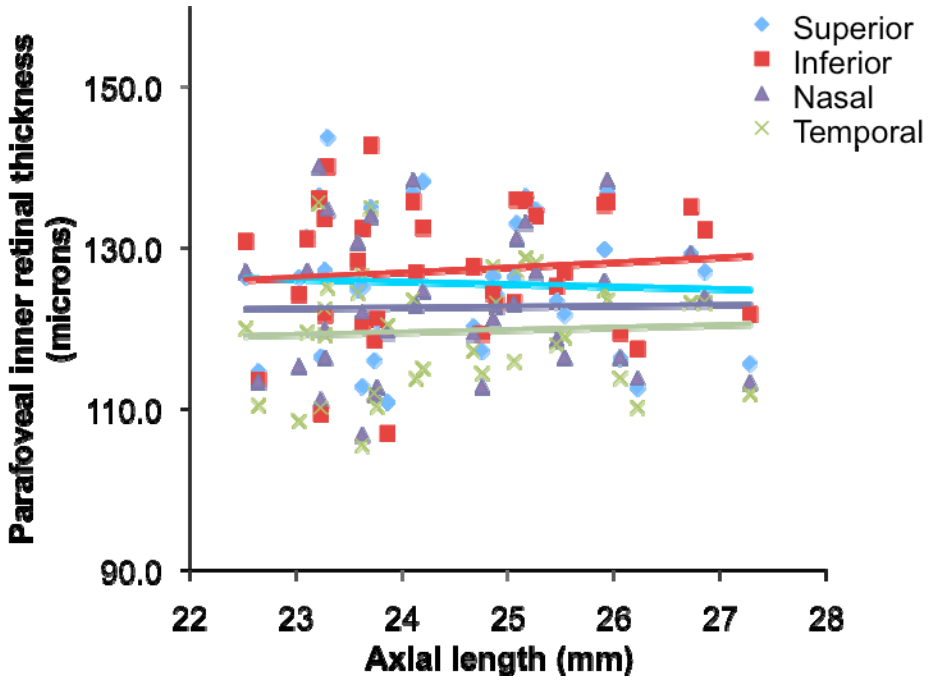


Fig. 3.4. Parafoveal (1-3 mm) inner retinal thickness and axial length by retinal quadrant.

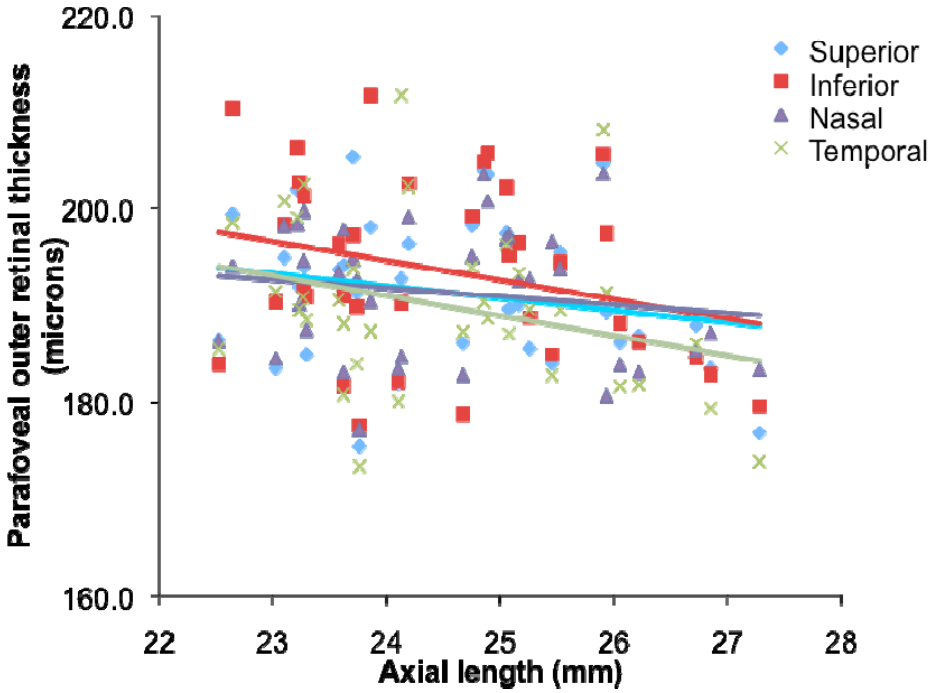


Fig. 3.5. Parafoveal (1-3 mm) outer retinal thickness and axial length by retinal quadrant.

In the perifoveal region (3-6 mm ring), full retinal thickness was greatest in the nasal quadrant and least in the superior quadrant. Full retinal thickness decreased with increasing axial length in all quadrants, and at a similar slope (Fig. 3.5). Without adjustment for eye size, this effect was significant in all four retinal quadrants, superior ($p=0.006$; $r^2=0.200$), inferior ($p=0.007$; $r^2=0.193$), nasal ($p=0.029$; $r^2=0.132$), and temporal ($p=0.028$; $r^2=0.134$). With adjustment for eye size, the respective p-values for full thickness regression against axial length became: superior ($p=0.022$), inferior ($p=0.023$), nasal ($p=0.075$), and temporal ($p=0.072$).

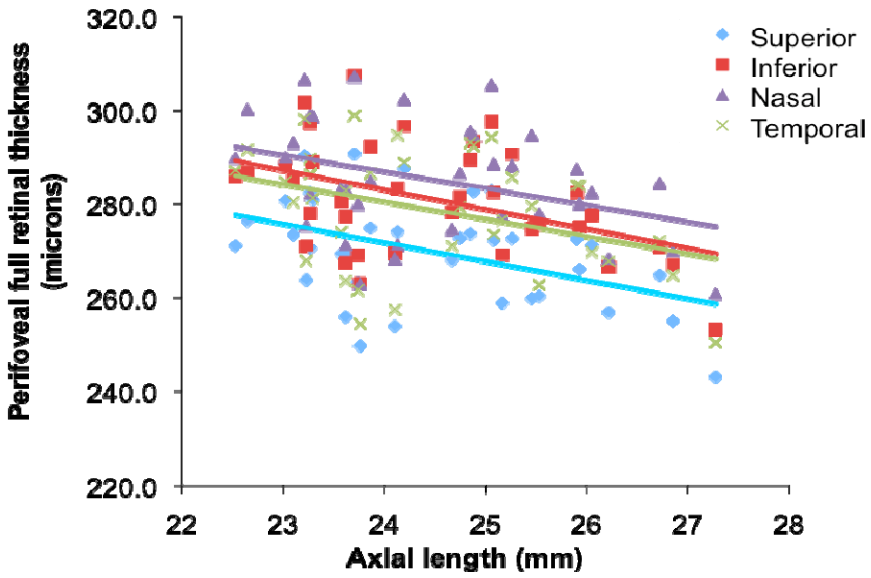


Fig. 3.6. Perifoveal (3-6 mm) full retinal thickness (unadjusted) and axial length by retinal quadrant.

Thus, the marginally significant relationships between full retinal thickness and axial length in the nasal and temporal quadrants became non-significant after adjustment

for eye size. The relative thickness of the inner and outer retinal layers changes with distance from the fovea, so the magnification adjustment may have a different effect on the inner and outer retinal layer thickness than on the full retinal thickness. Since the effect of the magnification adjustment has not been studied for the inner or outer retinal layer thicknesses, the remaining data are reported for the unadjusted thicknesses, with the caveat that adjustment for eye size could alter the significance of reported relationships.

The inner perifoveal retinal layer was overall thinnest in the superior quadrant and thickest in the nasal and inferior quadrants. The inner retinal layers became thinner with increasing axial length in all quadrants (Fig. 3.6). This slope was shallowest nasally and steepest superiorly; the superior quadrant showed significant inner retinal thinning with increasing axial length ($p=0.005$; $r^2=0.209$), but the effect was not statistically significant in any other quadrant. The outer retinal layers in the perifovea thinned significantly with axial length in all four retinal quadrants (Fig. 3.7): superior ($p=0.037$; $r^2=0.121$), inferior ($p=0.008$; $r^2=0.187$), nasal ($p=0.028$; $r^2=0.135$), and temporal ($p=0.040$; $r^2=0.119$). This effect was shallowest superiorly.

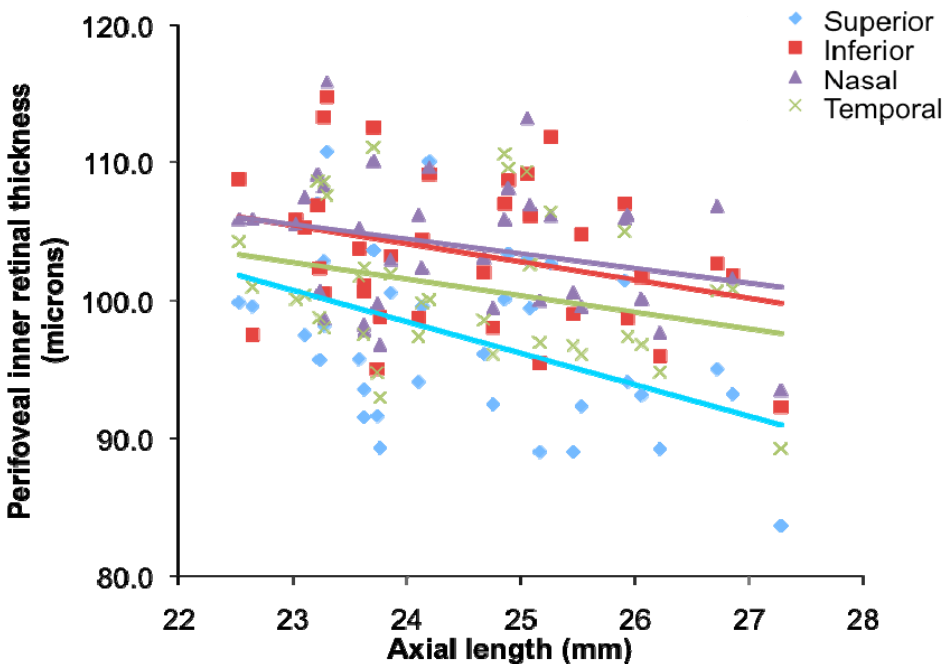


Fig. 3.7. Perifoveal (3-6 mm) inner retinal thickness and axial length by retinal quadrant.

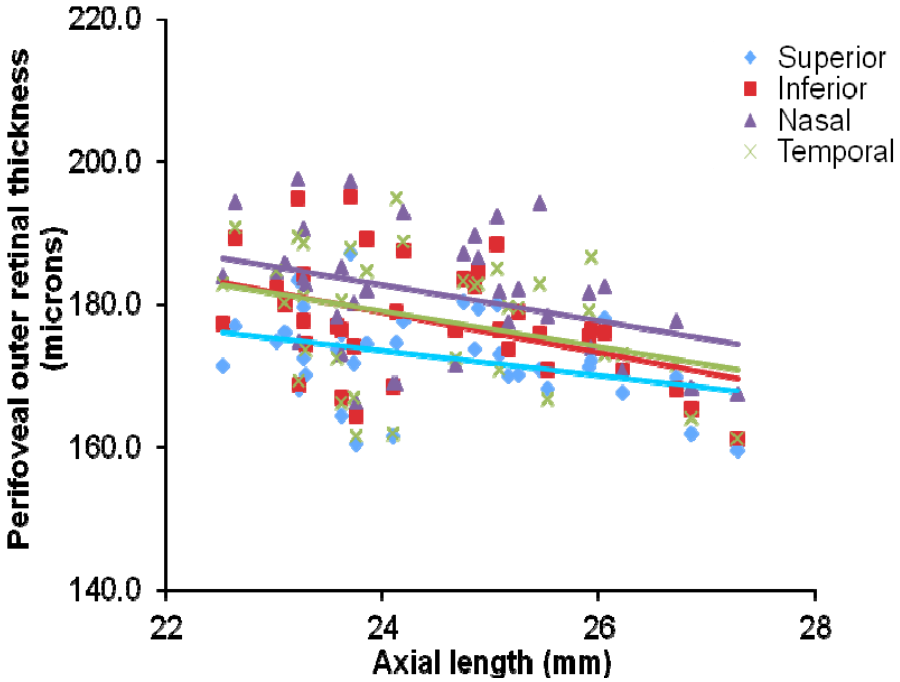


Fig. 3.8. Perifoveal (3-6 mm) outer retinal thickness and axial length by retinal quadrant.

3.3 Ratios of retinal layer thickness vs. axial length

The ratios of inner retinal thickness/full retina thickness and outer retinal thickness/full retinal thickness were plotted to investigate whether there were relative changes in the thickness of specific retinal layers against axial length in the parafoveal and perifoveal regions. This type of analysis examining relative thinning of particular retinal layers with myopia has generally not been done in previous OCT macular studies. In the parafovea, the inner retinal layer was about 40% while outer layer was about 60% of the full retinal thickness. There was no statistically significant change in the inner/full (Fig. 3.9) or outer/full (Fig. 3.10) thickness ratios in any retinal quadrant against axial length. However, as seen in Fig. 3.10, there was a trend for the parafoveal outer/full thickness ratio to decrease as axial length increased. This is consistent with the trends seen in the outer retinal layer thickness in Fig. 3.4.

In the perifovea, the inner retinal layer became proportionally thinner than in the parafoveal region, with the inner layer being about 36% and the outer layer being about 64% of the full retinal thickness. Layer ratios in the superior perifoveal quadrant showed a different pattern of variation against axial length than the ratios in the other three quadrants. In the superior quadrant, the inner/full retinal thickness ratio decreased significantly with axial length ($p=0.047$; $r^2=0.111$; Fig 3.11) and to correspond, the outer/full retinal thickness ratio increased significantly with axial length ($p=0.048$; $r^2=0.110$; Fig. 3.12). There was no statistically significant change in the inner/full or outer/full thickness ratios against axial length in the inferior, nasal, or temporal retinal quadrants, although the ratios tended to change in a similar fashion to those in the

parafoveal region. These results indicate that the inner retinal layer becomes proportionally thinner in the superior perifoveal retina with increasing axial length.

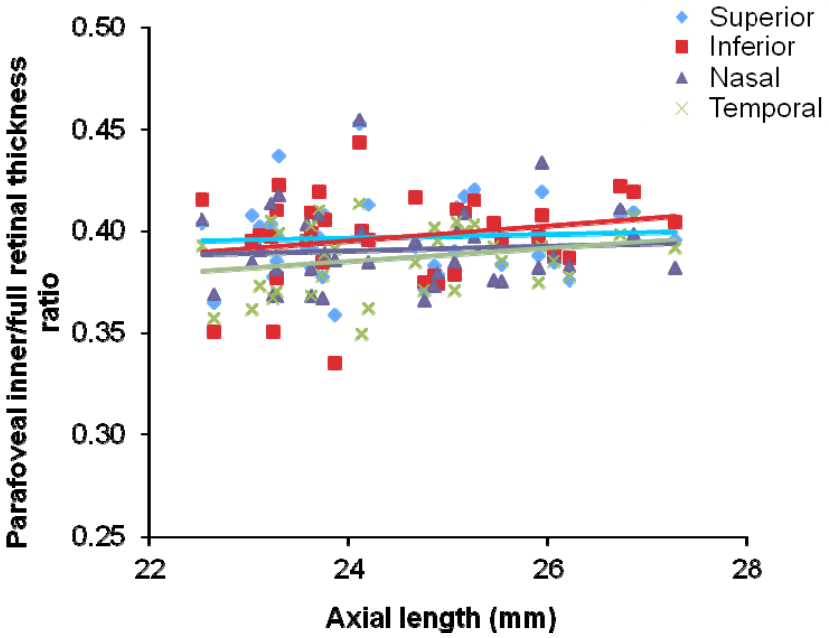


Fig.3.9. Parafoveal (1-3 mm) inner/full retinal thickness ratio and axial length by retinal quadrant.

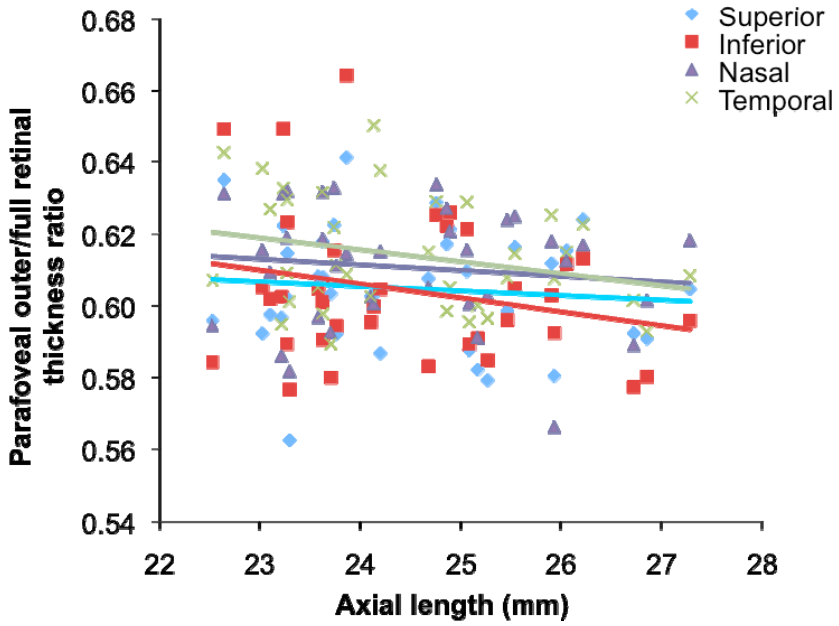


Fig. 3.10. Parafoveal (1-3 mm) outer/full retinal thickness ratio and axial length by retinal quadrant.

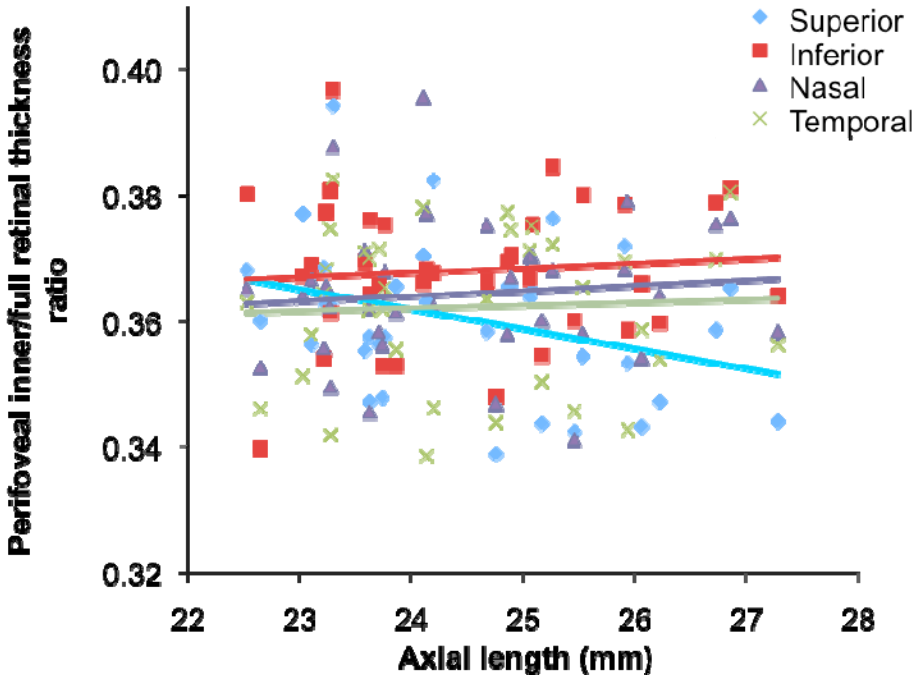


Fig. 3.11. Perifoveal (3-6 mm) inner/full retinal thickness ratio and axial length by retinal quadrant.

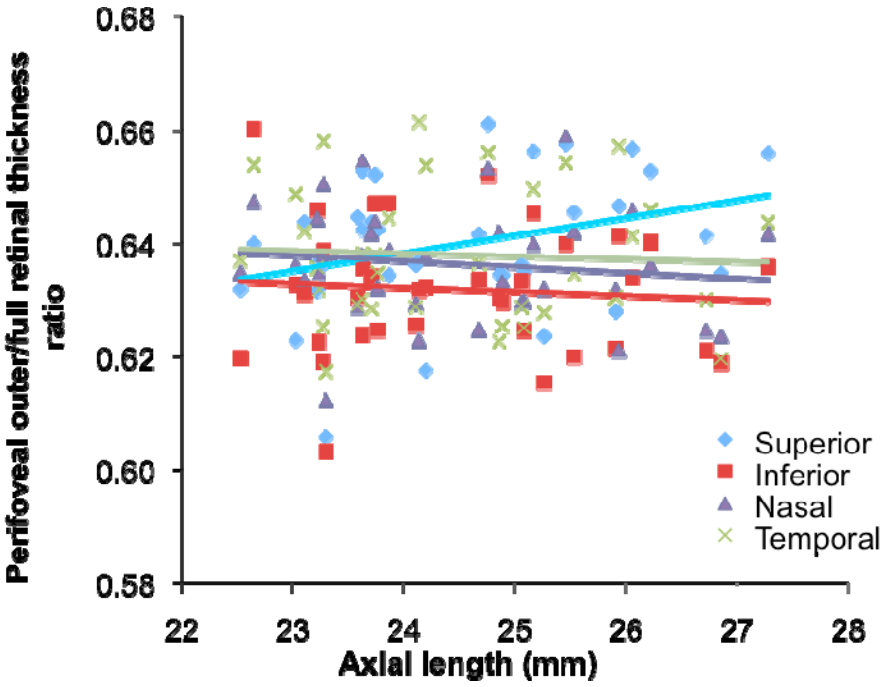


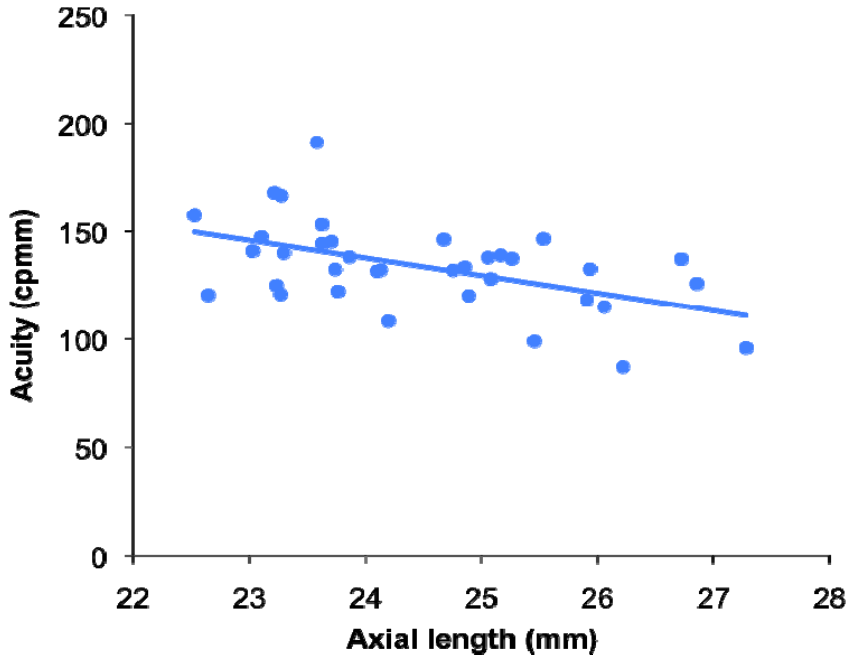
Fig. 3.12. Perifoveal (3-6 mm) outer/full retinal thickness ratio and axial length by retinal quadrant.

3.4 Retinal acuity and axial length

Interferometric acuity was converted to retinal acuity in cycles/mm to equate the stimuli on the retina. Since long eyes would magnify the retinal image, this conversion makes the acuity result independent of the eye's magnification characteristics (Coletta and Watson, 2006). Retinal acuity at the fovea decreased with increasing axial length ($p=0.001$; $r^2=0.261$; Fig. 3.13a), and with increasing myopia ($p<0.001$; $r^2=0.389$; Fig. 3.13b), as expected.

In the perifovea (Fig. 3.14), acuity is higher on the horizontal meridian (nasal and temporal locations) than on the vertical meridian (superior and inferior locations). The retinal acuity in all four perifoveal locations decreased with increasing axial length (Fig. 3.14a). The slope against axial length was similar between the inferior and superior meridians, and similar between the nasal and temporal meridians. The slopes were steeper in the horizontal meridian compared to the vertical. The reduction in acuity with increasing axial length was significant in the inferior ($p=0.044$; $r^2=0.114$), nasal ($p=0.018$; $r^2=0.153$), and temporal ($p=0.044$; $r^2=0.114$) retinal locations. Similar effects were seen with refractive error (Fig. 3.14b), with acuity decreasing with increasing myopia in all four retinal locations, although only statistically significant nasally ($p=0.019$; $r^2=0.151$).

(a)



(b)

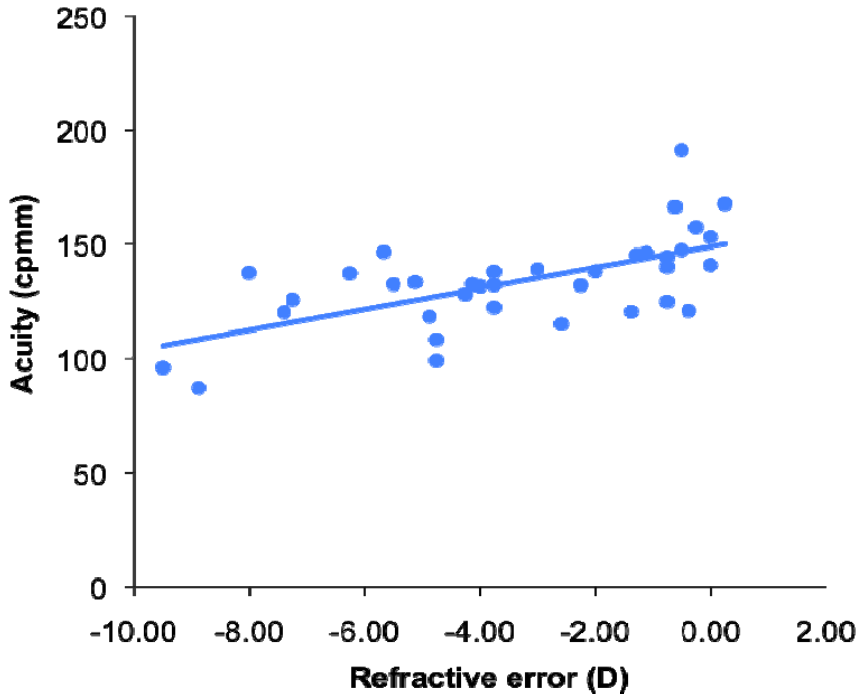


Fig. 3.13. Foveal retinal acuity as a function of axial length (a) and refractive error (b).

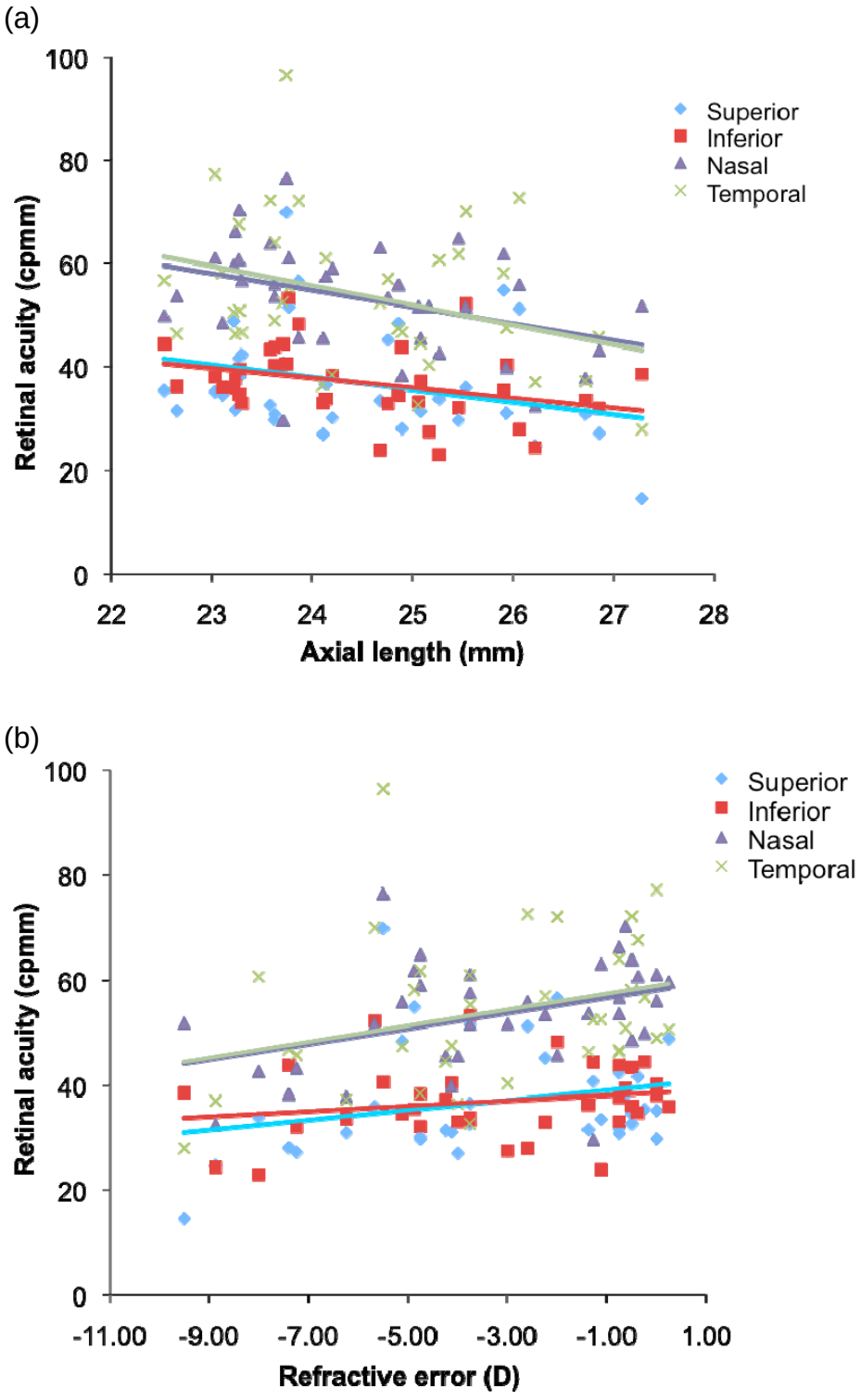


Fig. 3.14 Perifoveal retinal acuity as a function of axial length (a) and refractive error (b) by retinal quadrant.

3.5 Retinal acuity and retinal thickness

The relationship between retinal acuity and full, inner, and outer retinal thickness was examined for each perifoveal retinal quadrant; these plots are shown in Figures 3.15-3.17. The relationship between acuity and retinal thickness was not the same in each quadrant. Acuity was not associated with retinal thickness in any quadrant, but approached statistical significance in the superior quadrant. In the superior quadrant, acuity increased as full and outer retinal thickness increased (Figs. 3.15 and 3.17), approaching statistical significance ($p=0.086$; $r^2=0.084$ and $p=0.080$; $r^2=0.088$, respectively).

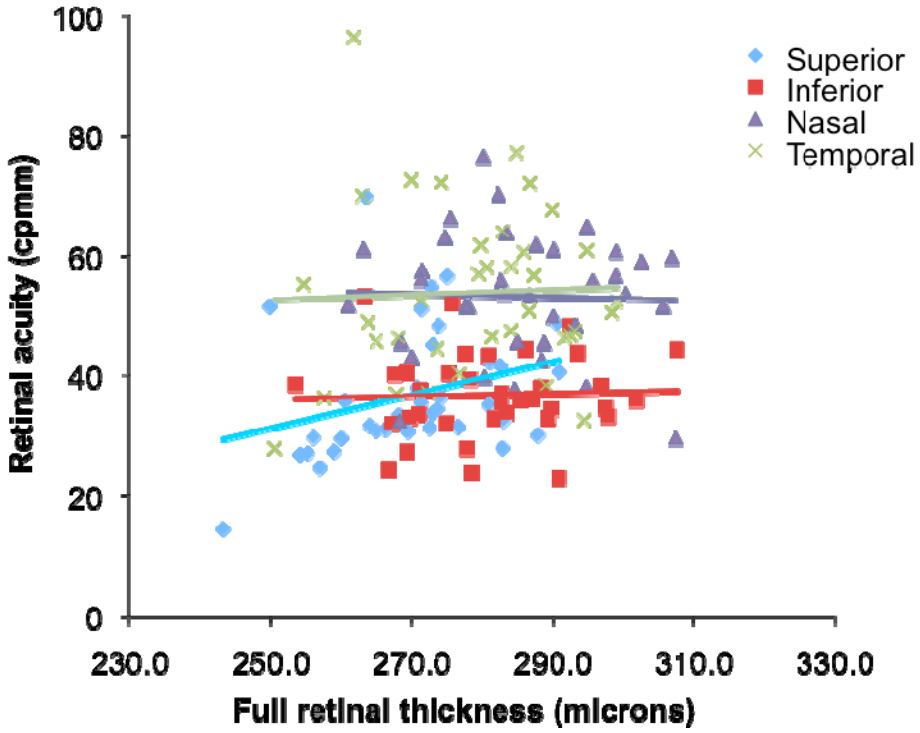


Fig. 3.15. Perifoveal full retinal thickness and acuity by retinal quadrant.

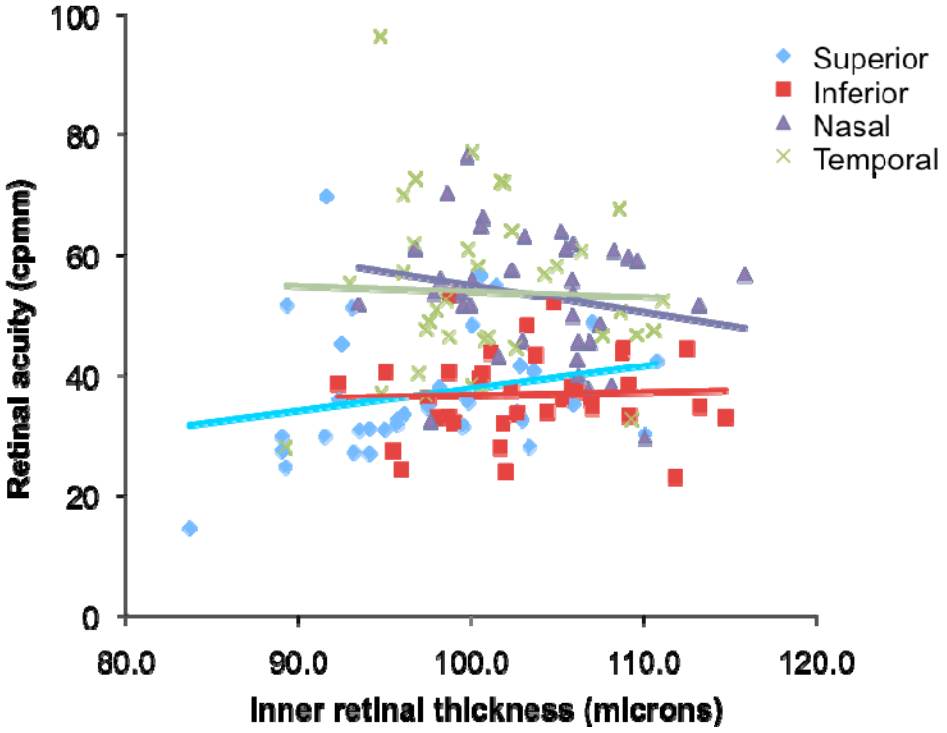


Fig. 3.16. Perifoveal inner retinal thickness and acuity by retinal quadrant.

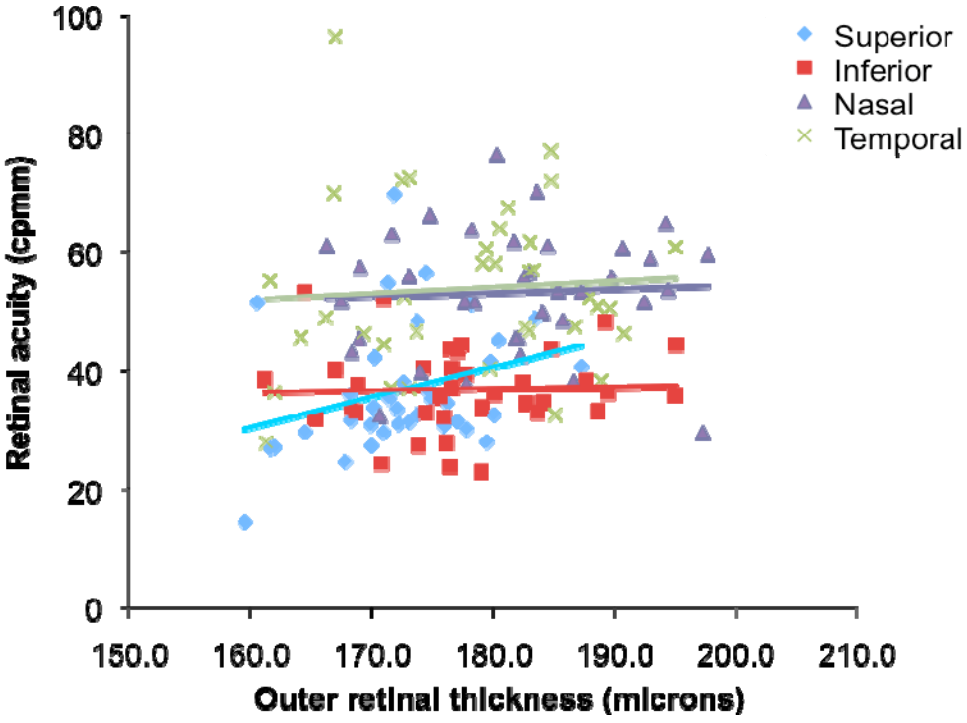


Fig. 3.17. Perifoveal outer retinal thickness and acuity by retinal quadrant.

The relationship between the retinal layer thickness ratios and retinal acuity was also examined in the four retinal quadrants (Figs. 3.18-3.19). In the nasal and temporal quadrants, retinal acuity tended to increase as the outer retinal layer proportionally increased in thickness, while acuity decreased as the inner/full thickness ratio increased. In other words, with proportional thickening of the outer retinal layers, retinal acuity on the horizontal meridian improved. These observed effects on the horizontal meridian were not statistically significant, however, and the significant amount of scatter in the data must be taken into consideration. With this in mind, the ratio results on the horizontal meridian are consistent with the idea that better acuity is associated with proportionally greater outer retinal layer thickness. In the superior and inferior quadrants, there is not much change in acuity against the layer thickness ratios, even though the superior retinal acuity increased with increasing thickness in all layers (Figs. 3.15-3.17).

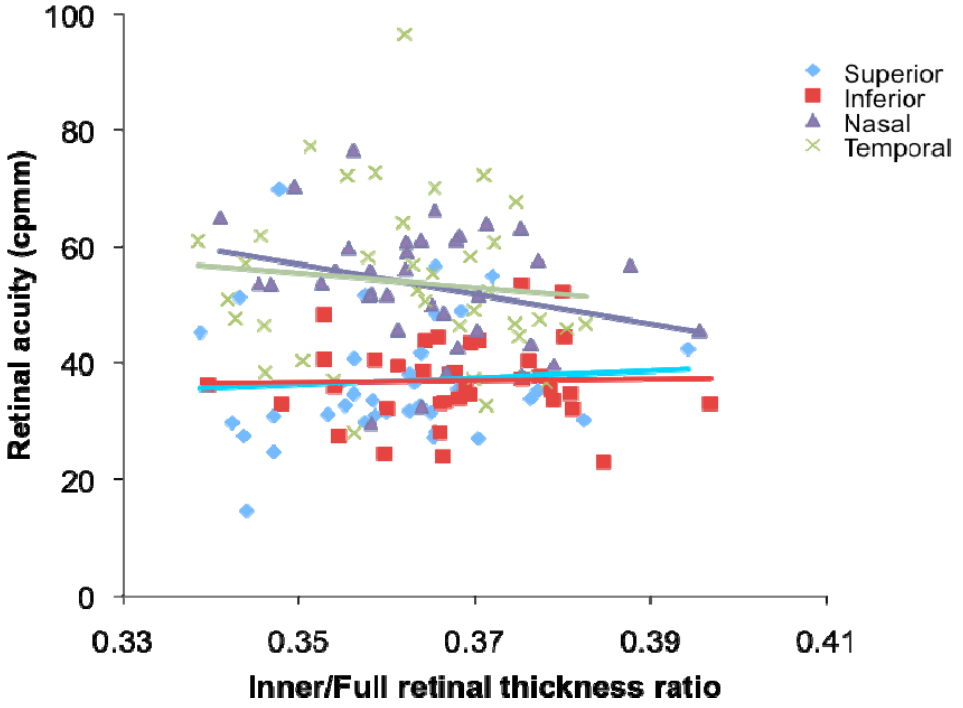


Fig. 3.18 Inner/full retinal thickness ratio and acuity by retinal quadrant.

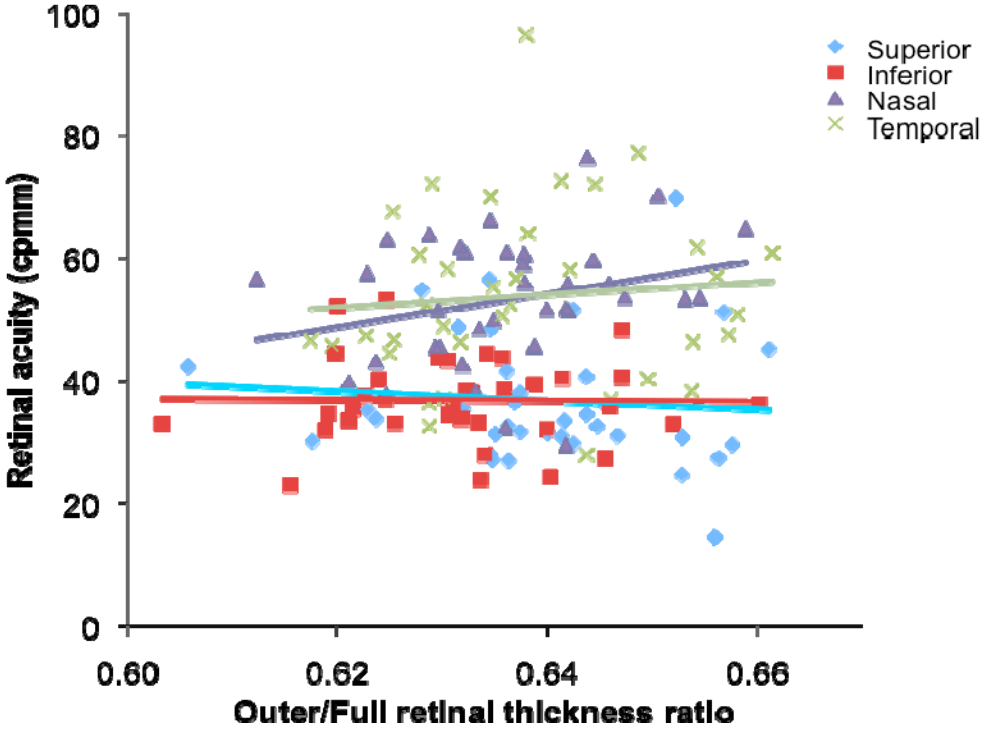


Fig. 3.19 Outer/full retinal thickness ratio and acuity by retinal quadrant.

4. Retinal Contour and Retinal Thickness

4.1 Biometric characteristics of the subjects

A total of 46 subjects were included in the analysis of retinal contour, ranging in age from 22 to 39 years with an average of 24.86 years ± 2.91 s.d. Retinal thickness measurements were also available on all of these subjects. Refractive errors ranged from +0.75 D to -9.50 D with less than 1.50 D astigmatism; average refraction was -3.29 D ± 2.82 s.d. Axial lengths ranged from 22.5 to 27.3 mm with an average of 24.52 mm ± 1.27 s.d. Central corneal power ranged from 40.6 to 47.3 D with an average of 44.3 D ± 1.52 s.d. Anterior chamber depth ranged from 2.17 to 4.19 mm with an average of 3.28 mm ± 0.66 s.d.

4.2 Retinal contours

As stated in the Methods section, subjects were divided into four refractive groups to visualize how retinal contours varied with refractive error. The emmetropic group included 13 subjects with refractive error between +0.75 D and -0.75 D (average=-0.27 D ± 0.49 s.d.). The low myopic group included 10 subjects with refractions ranging from -1.00 D to -3.00 D (average=-1.70 D ± 0.56 s.d.). Moderate myopes included 14 subjects with refractive error ranging from -3.00 D to -6.00 D (average=-4.45 D ± 0.77 s.d.), and the high myope group included 9 subjects with refractive errors of more than -6.00 D of myopia (average=-7.62 D ± 1.25 s.d.).

Retinal contours in the horizontal and vertical meridians were first visualized for each refractive group by plotting average retinal depth coordinates (s_r in Fig. 2.4) by retinal eccentricity in degrees. As measurements could not be attained for all subjects beyond 30 degrees eccentricity in each meridian due to pupil size, the retinal contour curve was only extended out to 30 degrees. Data beyond 30 degrees are displayed for lower numbers of subjects in each group and are shown as a scatter plot. Results for the vertical meridian are shown in Figure 4.1 and results for the horizontal meridian are shown in Fig. 4.2.

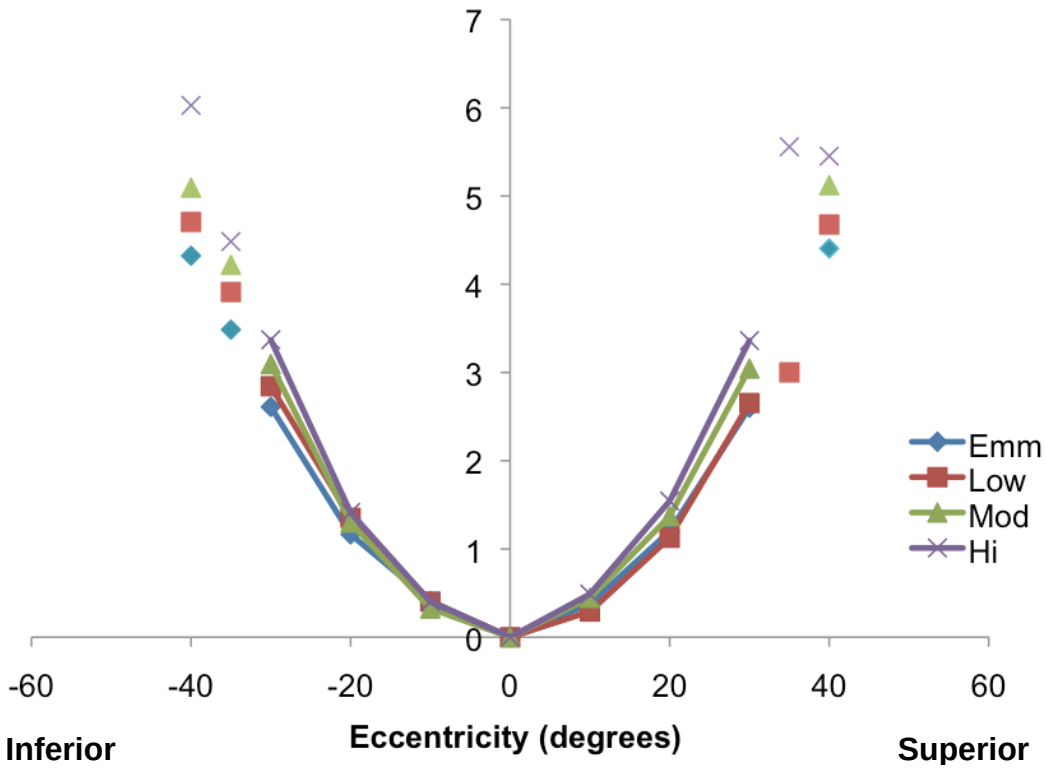


Fig. 4.1. Vertical depth coordinates in mm and retinal eccentricity in degrees, indicating retinal contour in the inferior (negative degrees) and superior (positive degrees) retinal meridians.

In the inferior meridian, the highly myopic group showed the steepest retinal contour followed by the moderate myopes, low myopes, and emmetropes, respectively. This differentiation in retinal contour in the inferior meridian was most evident beyond 20 degrees eccentricity. In the superior meridian, the highly myopic group showed the greatest retinal steepness followed by the moderately myopic group. The low myope and emmetrope groups showed similar retinal contours in the superior meridian.

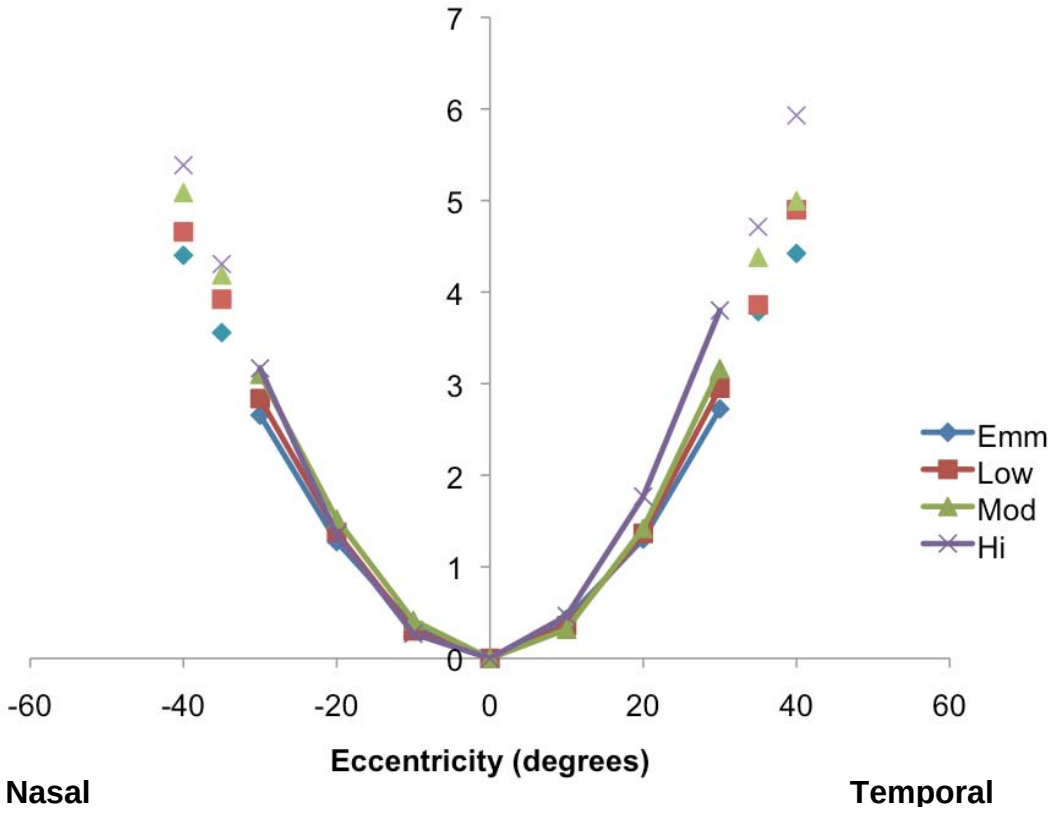


Fig. 4.2. Horizontal depth coordinates in mm and retinal eccentricity in degrees, indicating retinal contour in the nasal (negative degrees) and temporal (positive degrees) retinal meridians.

In the nasal retinal meridian (Fig. 4.2), all four refractive groups showed similar retinal contour. In the temporal meridian, the highly myopic group showed a notably steeper retinal contour than all other refractive groups beyond 10 degrees eccentricity. The emmetropic, low myopic, and moderately myopic groups had similar retinal contours in the temporal meridian.

To investigate asymmetries in retinal contour in the horizontal and vertical meridians, paired t-tests were done comparing the retinal depth coordinates in opposing sides of a meridian in each refractive group. Retinal depth coordinates in the inferior meridian were compared to those in the superior meridian, and the nasal depth coordinates were compared to those in the temporal meridian. Plots are shown for eccentricities of 10, 20 and 30 degrees in Figures 4.3 and 4.4. Depth increases with eccentricity, so all plots have the same vertical scale range of 1.4 mm for better comparison of trends at each eccentricity.

In the vertical meridian, as seen in Figure 4.3, the moderately myopic group showed a significant asymmetry at 10 degrees eccentricity with the superior depth being greater than the inferior depth ($p=0.046$). At this eccentricity, the moderate and high myopes had greater depth on the superior meridian, while emmetropes and low myopes had greater depth on the inferior meridian. At 20 deg eccentricity, the latter trend was still apparent and there was a significantly greater inferior depth for the low myope group ($p=0.005$). At 30 degrees eccentricity, inferior meridian depth tended to be greater in all refractive groups and was significantly greater ($p=0.015$) for the low myope group.

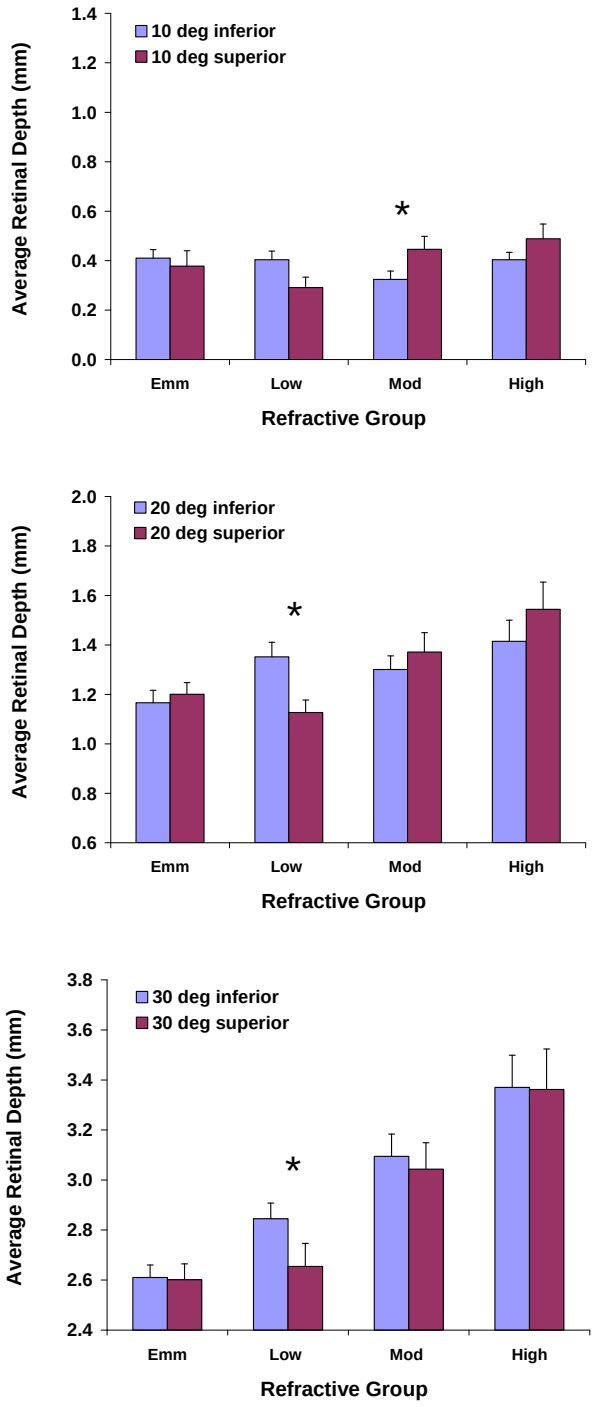


Fig. 4.3. Average retinal depth in mm at 10, 20 and 30 degrees eccentricity in the inferior and superior retinal meridian, by refractive group. All vertical scales span a retinal depth range of 1.4 mm. Error bars are 1 s.e.m. Asterisks indicate $p<0.05$ in paired t-test.

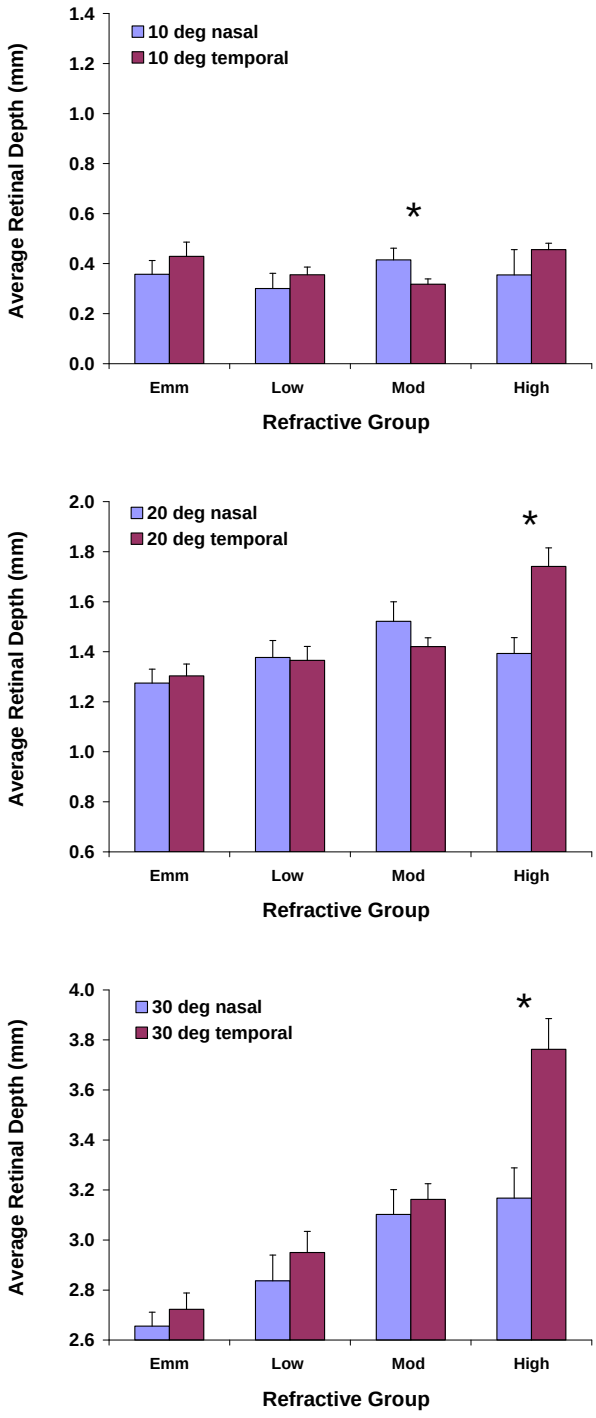


Fig. 4.4. Average retinal depth in mm at 10, 20 and 30 degrees eccentricity in the nasal and temporal retinal meridian, by refractive group. Vertical scales span a retinal depth range of 1.4 mm. Error bars are 1 s.e.m. Asterisks indicate $p<0.05$ in paired t-test.

In the horizontal meridian, as seen in Figure 4.4, the main trend is that the high myopes demonstrate asymmetry, with the temporal meridian showing significantly greater retinal depth than the nasal meridian at 20 degrees ($p=0.004$) and at 30 degrees ($p<0.001$). Other refractive groups also have a tendency to have greater depth on the temporal side at 30 degrees, but this effect is not observed at 20 degrees where the nasal depth is greater for all groups but the high myopes. At 10 degrees eccentricity, the moderately myopic group showed a significantly greater depth on the nasal meridian ($p=0.01$).

The asymmetries in retinal contour at 20 and 30 deg eccentricity indicate that low myopes have a more anterior retinal position inferiorly than superiorly, while high myopes have a more anterior retinal position temporally than nasally. Differences in retinal thickness on either side of the fovea would not account for these results, because the IOL Master measurement is based on reflection of light at the retinal pigment epithelium. Furthermore, the asymmetries in peripheral retinal contours at 10 deg are on the order of tenths of millimeters which is much larger than the measured differences in retinal thickness between opposing perifoveal quadrants reported in Chapter 3, which are on the order of several microns. Differences in choroidal thickness similarly would not be expected to explain these asymmetries as regional variations in choroidal thickness have been reported to be on the order of microns (Flores-Moreno et al, 2013).

The differences in retinal depth most likely indicate differences in eye shape. The nasal-temporal asymmetry in high myopes is consistent with other reports (Logan et al., 2004; Ehsaei et al., 2013); this result has been interpreted as evidence for greater expansion of the myopic globe in the posterior direction on the nasal side of the fovea,

such that the nasal retina is further back than the corresponding temporal retina. This asymmetry in high myopes is also consistent with a report of more peripheral hyperopia on the temporal side in myopes (Chen et al. (2010). The asymmetry observed on the vertical meridian in the periphery in low myopes (Fig. 4.3), with the inferior retina in a relatively more anterior position than the superior retina, may also indicate that the superior retina undergoes greater stretching than the inferior retina in that refractive group. This effect should result in greater relative peripheral hyperopia for the inferior retina than the superior retina in low myopes. This asymmetry, although not observed in all myopes, may be consistent with the retinal thinning in the superior region observed in Chapter 3.

4.3 Retinal contour by linear retinal eccentricity

Published studies of peripheral retinal contour have used angular units of eccentricity to compare eye shapes among different refractive groups (Ehsaei et al., 2013; Mallen and Kashyap, 2007; Logan et al., 2004). When data from different eye sizes are compared in angular units of eccentricity, the eye size affects the retinal position of the peripheral measurement. That is, 30 degrees eccentricity in a long eye is further away from the fovea than 30 degrees in a short eye.

In order to compare retinal contour data at the same retinal locations, rather than at the same angular positions, retinal contour was also plotted against the linear retinal eccentricity coordinates, in mm, calculated from the scheme outlined in the Methods section (y_r in Fig. 2.4). These results for the vertical meridian, shown in the upper panels of Fig. 4.5, indicate that plotting both depth and eccentricity coordinates on linear scales

makes the retinal contours more similar for all refractive groups. However, the low myopes still exhibit an asymmetry on the vertical meridian in which the inferior retinal position is more forward (greater depth or steeper contour) than the superior retinal position. The low myope group also has a steeper inferior retinal position and shallower superior retinal position compared to the other refractive groups. The shallower retinal position on the superior side in low myopes could indicate that the myopic eye has grown more on the superior meridian, i.e., it is relatively further back, than on the inferior side. This could mean that there is more retinal stretching in the superior retina than in the inferior retina.

Results for the horizontal meridian, shown in the lower panels of Fig. 4.5, indicate that the high myope group still exhibited a nasal-temporal asymmetry in which the temporal retinal position is more forward (steeper contour) compared to the nasal retina. The high myope group also has a shallower nasal retinal position and steeper temporal retinal position compared to the other refractive groups. The shallower retinal position on the nasal side in high myopes could indicate that the myopic eye has grown more on the nasal side, i.e., it is relatively further back, than on the temporal side. This could mean that there is more retinal stretching on the nasal side than on the temporal side.

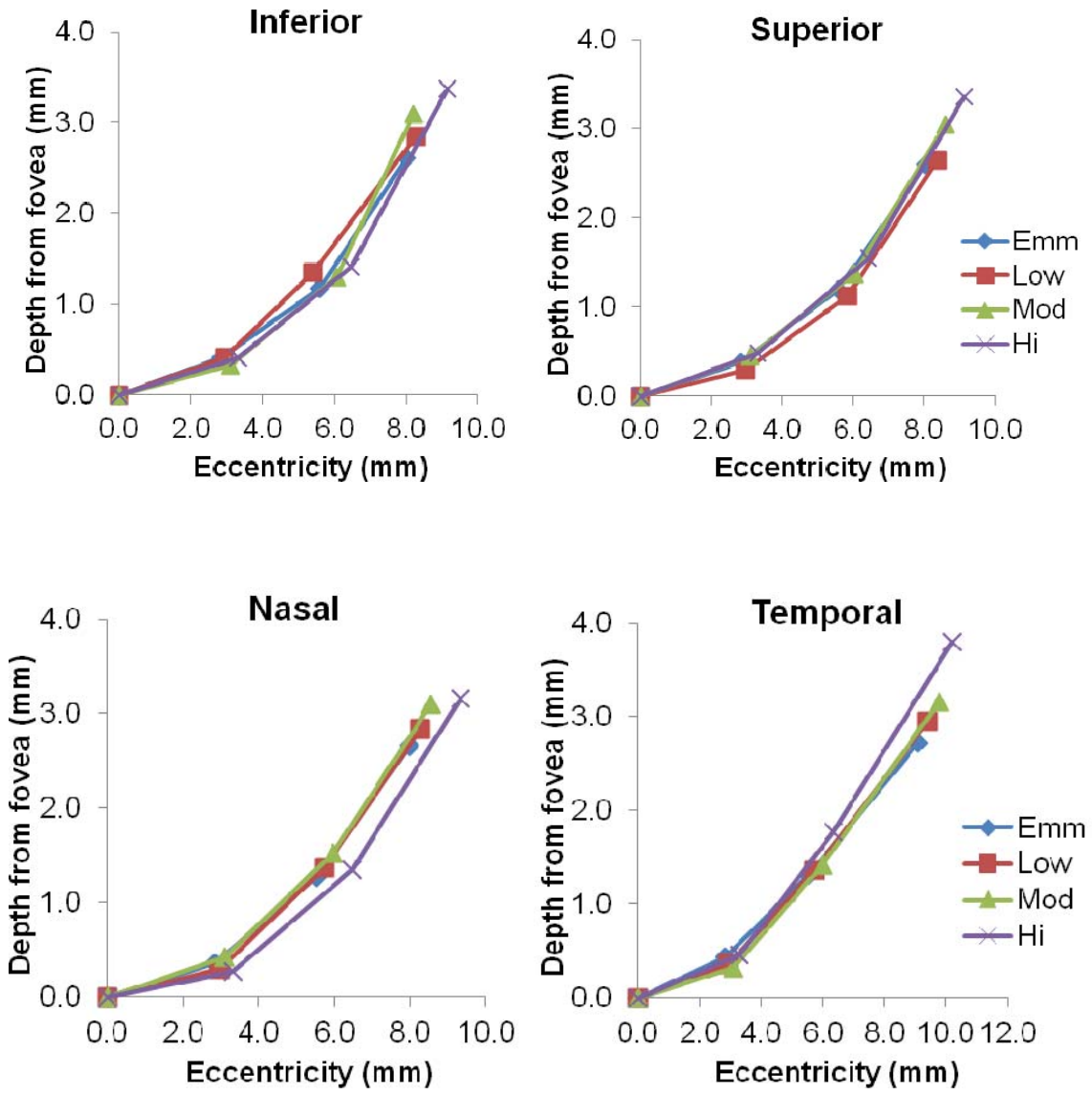


Fig. 4.5. Retinal depth coordinates, in mm, in the vertical (upper panels) and horizontal meridians (lower panels) plotted by retinal eccentricity in millimeters.

4.4 Comparison of results to a published study

A recent study compared peripheral axial length readings from the IOL Master in emmetropes and myopes (Ehsaei et al., 2013). Their study plotted the relative peripheral eye length for angular eccentricities from 0 to 30 deg. In this type of plot, the central axial length is subtracted from the distance *p* plus *q* in Fig. 2.4, and the resulting difference is plotted as a function of eccentricity angle. It should be noted that these types of plots are not actual retinal contours, as were calculated from the retinal s_r and y_r coordinates in this study, because the differences in peripheral eye lengths are all relative to the corneal position which does not lie in a plane. Ehsaei et al., 2013 reported that relative peripheral eye lengths at 30 deg were about -0.3 mm in emmetropes and as much as -1 mm in myopes. Emmetropes had no asymmetries in peripheral axial lengths. Myopes had a significant asymmetry at 30 deg, with the temporal retina being in a relatively more anterior position than the nasal retina, but there was no difference in peripheral eye lengths for the inferior vs. superior meridians in myopes.

Relative peripheral eye lengths from the current study are plotted in Figure 4.6. Since the data from myopes in the Ehsaei et al., 2013 study spanned a large refractive range, the data from all the myopes in this study were combined. The average spherical equivalent refraction of the 33 myopes in this study was -4.42 D+/-2.4 D s.d. Data from the inferior and superior meridians are shown on the top panel while data from the nasal and temporal meridians are shown on the lower panel in Fig. 4.6. IOL Master readings were generally shorter off-axis than centrally, so the relative peripheral eye lengths are negative. The relative peripheral eye lengths are fit well by second-order polynomial functions as shown.

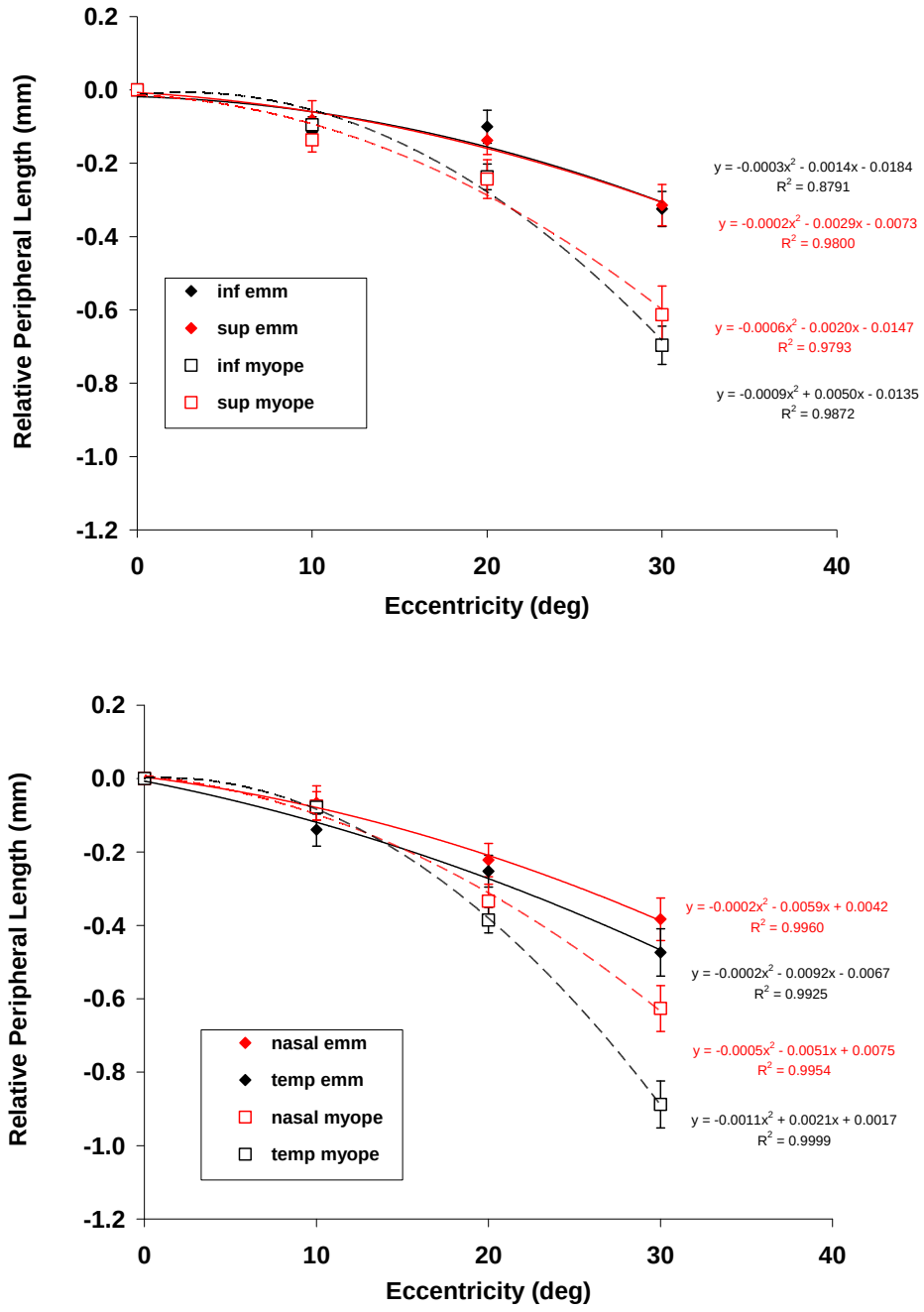


Fig. 4.6 Relative peripheral eye length, taken as the difference of the off-axis measurement minus the central axial length, plotted as a function of angular eccentricity for the inferior and superior meridians (top panel) and for the nasal and temporal meridians (lower panel).

Relative peripheral eye lengths in the current study are very similar to those reported in the Eshaei et al. study. Average values at 30 deg for myopes are in the range of -0.6 to -0.9 mm and, for emmetropes, are in the range of -0.3 to -0.4 mm. Myopes in the current study also show the large nasal-temporal asymmetry reported by Ehsaei et al., indicating a more anterior position of the temporal retina compared to the nasal retina. Comparing data from all four meridians at 30 deg, the temporal retina showed the greatest difference in peripheral eye length compared to the central axial length. When data from all myopes are grouped, there is no longer evidence for the inferior-superior asymmetry on the vertical meridian, observed here only in the low myopes (Fig. 4.3).

4.5 Retinal depth and axial length

The retinal depth coordinate calculated in this study represents the axial displacement of the peripheral retina relative to the foveal plane. It is an indicator of retinal steepness at the specified retinal eccentricity. As the vertical and horizontal retinal contour plots in Figs. 4.1 and 4.2 showed differentiation in retinal steepness beyond 20 degrees eccentricity generally, a regression analysis was done between retinal depth at 30 degrees eccentricity and axial length (upper panel of Fig. 4.7).

It was found that retinal depth coordinates (s_r) increased significantly with axial length at 30 degrees eccentricity in all four retinal quadrants, superior ($p<0.001$; $r^2=0.474$), inferior ($p<0.001$; $r^2=0.620$), nasal ($p<0.001$; $r^2=0.385$), and temporal ($p<0.001$; $r^2=0.690$). The greatest effect was seen in the temporal quadrant, while the smallest effect was seen in the nasal quadrant. The inferior and superior quadrants showed similar rates of change against axial length. Similar results were found between

retinal depth at 30 degrees and refractive error as seen in the lower panel of Figure 4.7. Retinal depth increased with increasing myopia, significant in all four retinal quadrants, superior ($p<0.001$; $r^2=0.444$), inferior ($p<0.001$; $r^2=0.513$), nasal ($p<0.001$; $r^2=0.330$), and temporal ($p<0.001$; $r^2=0.662$), with a greater slope temporally than nasally. These results indicate that the eye shape changes most rapidly with myopia on the temporal side of the fovea and least rapidly on the nasal side.

The OCT measures of retinal thickness were performed at eccentricities closer to the macula and within the eccentricity of the optic nerve head, so retinal depth coordinates recorded for 10 deg eccentricity were also examined as a function of axial length and refraction. These results are shown in Fig. 4.8. Generally, the retinal depth coordinates this close to the fovea did not vary systematically with axial length or refraction. However, there was a tendency for the superior retinal depth to increase with increasing axial length and increasing myopia. The regression of superior retinal depth coordinates at 10 deg against refraction was statistically significant ($p=0.035$; $r^2=0.097$). These data imply that myopia affects the relative position of the superior retinal meridian close to the fovea. The greater the axial length or higher the myopia, the more anterior is the position of the superior retinal meridian at 10 deg relative to the inferior meridian. Thus the regression lines in Fig. 4.8 are consistent with the asymmetry seen in the moderate and high myope refractive groups in Fig. 4.3 in which the superior retina is more anterior than the inferior retina.

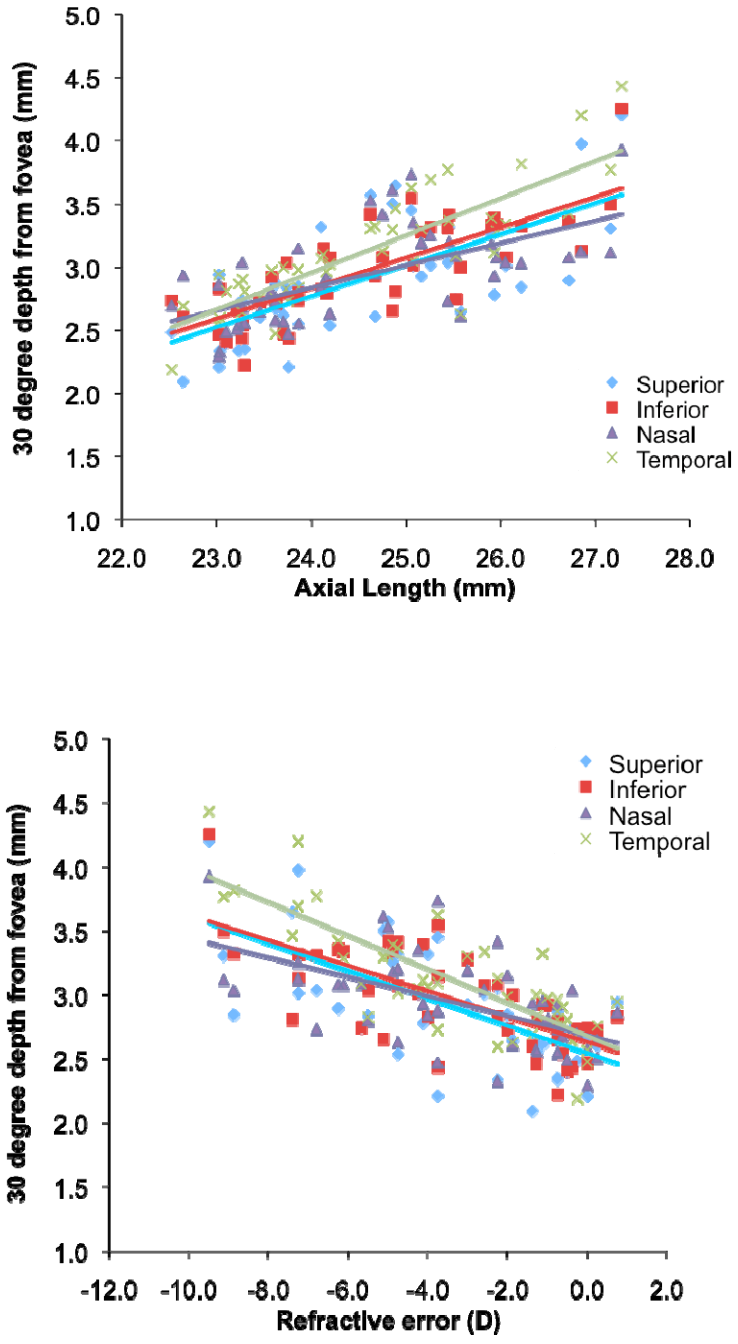


Fig. 4.7. Retinal depth coordinates at 30 degrees eccentricity by axial length (top panel) and refraction (lower panel) in four retinal quadrants.

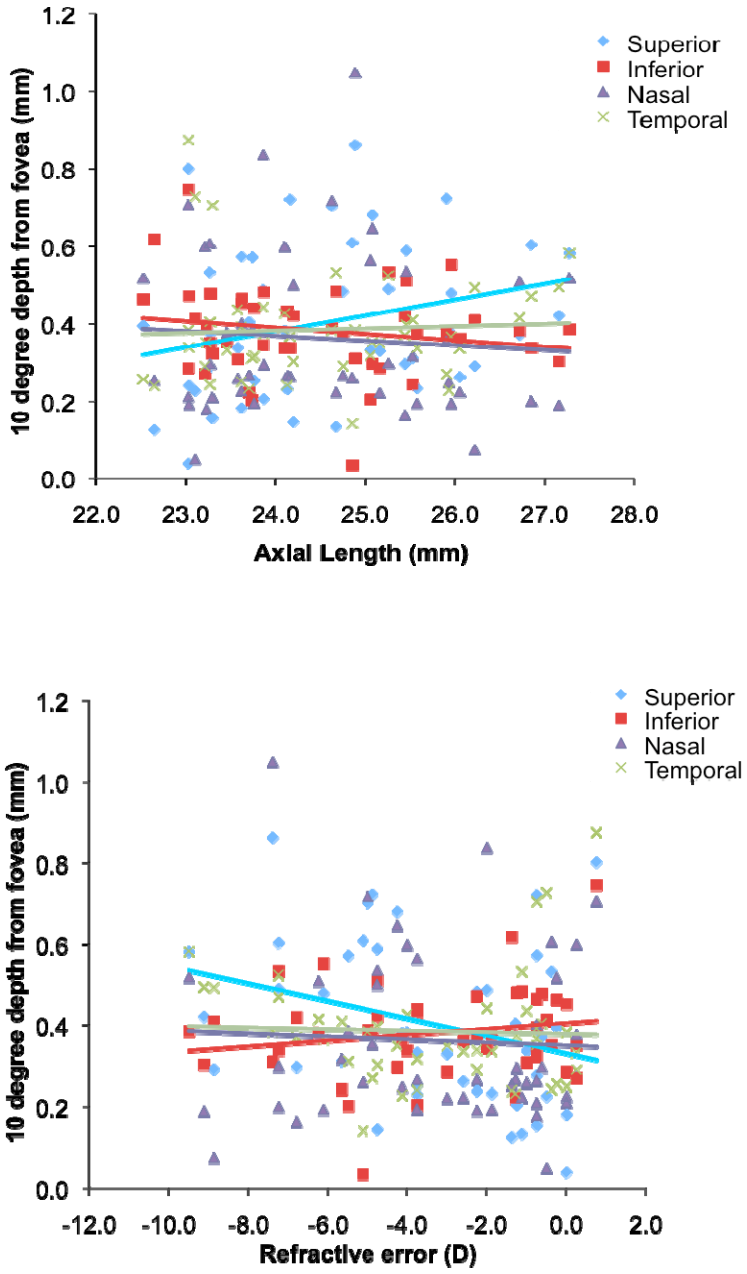


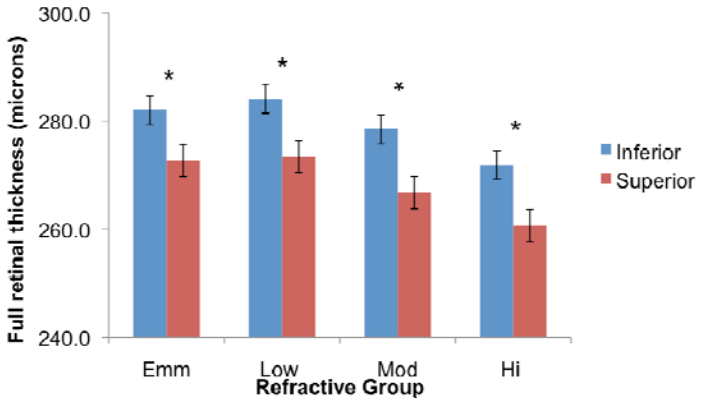
Fig. 4.8. Retinal depth coordinates at 10 degrees eccentricity by axial length (top panel) and refraction (lower panel) in four retinal quadrants.

4.6 Retinal thickness and retinal contour

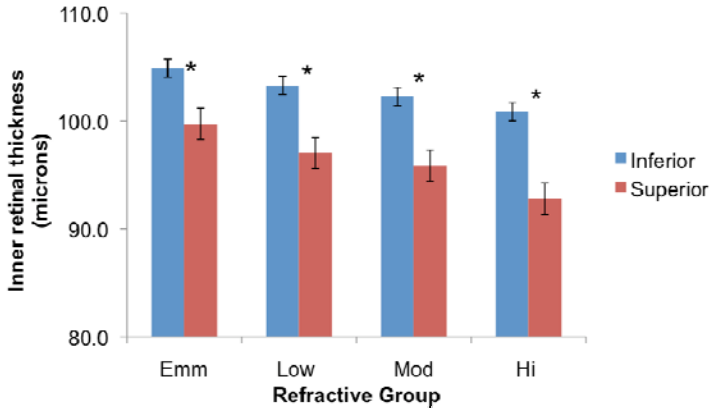
An analysis was done to investigate whether retinal thickness, as measured by OCT, correlated with retinal shape in each quadrant. We were interested in whether retinal shape changes in the periphery were reflected in retinal thickness changes in the macular region. Since myopes have greater retinal depth coordinates and retinal thinning, one might expect that thinner perifoveal retina would be associated with greater retinal depth coordinates. On the other hand, the literature has interpreted shallower retinal depth on a given side of the fovea as evidence for greater eye growth, and hence this might be expected to associate with retinal thinning.

Retinal thickness in the perifovea was first compared in the vertical and horizontal meridians for the four refractive groups in order to determine whether the meridional asymmetries exhibited in retinal contour corresponded with asymmetries in retinal thickness. The thickness data were obtained from all the subjects who participated in the retinal contour measurements. Paired t-test analysis was done for each refractive group comparing the inferior to superior meridian, and the nasal to the temporal meridian. Full, inner, and outer retinal thickness measurements were each analyzed. Figure 4.9 shows the averaged perifoveal retinal thickness grouped according to the subjects' refractive errors. The inferior perifoveal region was consistently thicker than the superior perifoveal region in all refractive groups, true for full, inner, and outer retinal thickness. The main effect that is associated with increasing myopia is the thinning of the inner retina in the superior meridian, evident in the middle panel of Fig. 4.9.

(a)



(b)



(c)

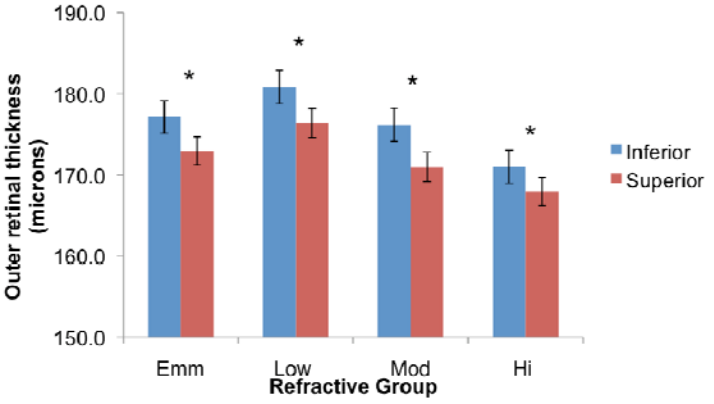
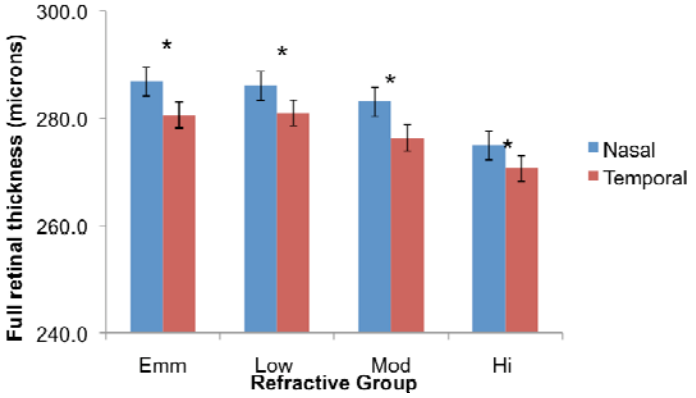
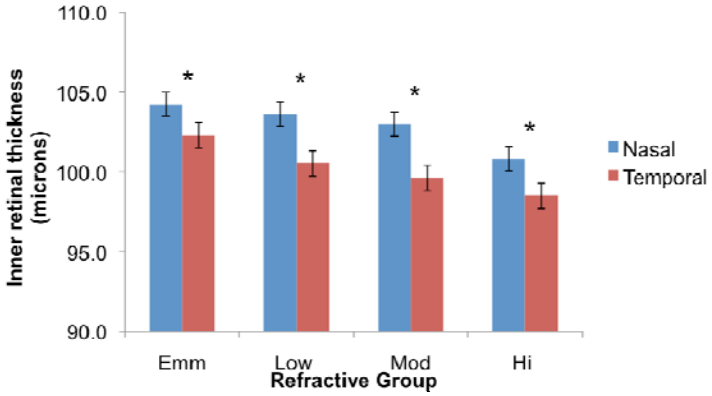


Fig. 4.9 Perifoveal retinal thickness in the inferior and superior retinal meridian by refractive group. Average full (a), inner (b), and outer (c) retinal thickness are plotted independently for each refractive group. Asterisks indicate $p<0.05$ in paired t-test.

(a)



(b)



(c)

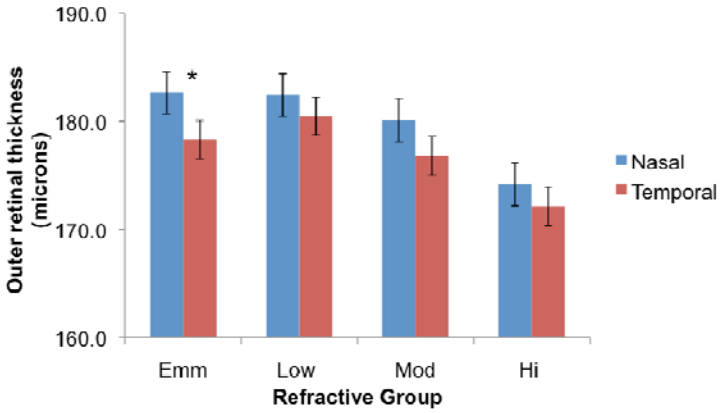


Fig. 4.10. Perifoveal retinal thickness in the nasal and temporal retinal meridian by refractive group. Average full (a), inner (b), and outer (c) retinal thickness are plotted independently for each refractive group. Asterisks indicate $p<0.05$ in paired t-test.

Inferior-superior retinal contour asymmetry was generally most pronounced for the low myope group at 20 and 30 deg eccentricity, in which the inferior retina had a significantly greater depth coordinate, or more anterior position, than the superior retina (Fig. 4.3). At 30 deg, moderate and high myopes also had a tendency for greater depth on the inferior meridian. This result could imply greater eye growth in the posterior direction on the superior side of the fovea and this may be associated with the inner retinal thinning observed in the OCT data on the superior meridian. However, at 10 deg, which is closer to the region of the OCT measurements, retinal depth was greater superiorly than inferiorly for the moderate and high myopes (Fig. 4.3). Thus there is not a clear pattern suggesting that retinal thickness is associated with retinal depth or contour on the vertical meridian.

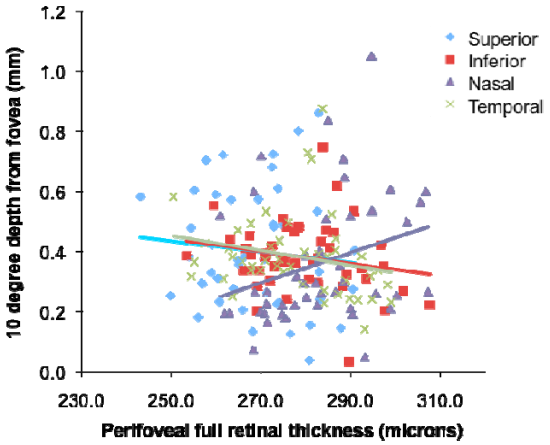
In the horizontal meridian (Fig. 4.10), perifoveal full, inner, and outer thickness was thicker nasally than temporally in all refractive groups; this effect was significant in all groups for full and inner retina but only for emmetropes in outer retina. As myopia increases, though, there is a tendency for relatively more thinning of the outer retina in both nasal and temporal retinal meridians (lower panel), but there isn't evidence for an asymmetry in this thinning, with one side thinning more than the other. The nasal-temporal asymmetry in retinal contour, with the temporal retina more anterior to the nasal retina, was mainly a feature of the periphery at 20 and 30 deg eccentricity and was mainly evident in the high myope group (Fig. 4.3). If the shallower depth of the nasal retina implies greater eye growth on the nasal side of the fovea, this result is not consistent with the thicker nasal retina in the perifovea. Only the moderate myopes exhibited the opposite effect in retinal contour at 10 deg and, to a lesser extent, 20 deg

(top and middle panels of Fig. 4.3) consistent with the OCT data, in which the nasal retina was anterior to the temporal retinal position.

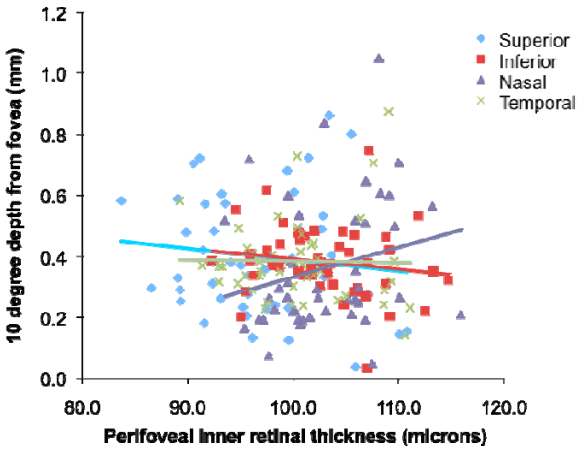
Regression analysis was performed correlating retinal thickness in the perifoveal region to retinal contour at 10 degrees eccentricity, as these locations correspond most closely. Full, inner, and outer retinal layer thickness were each analyzed separately (Fig. 4.11). Retinal depth coordinates in the superior, inferior, and temporal regions tended to decrease with increasing full perifoveal thickness (Fig. 4.11a), although none were statistically significant. The opposite trend is seen in the nasal region, in which retinal depth increased with increasing full retinal thickness ($p=0.049$; $r^2=0.086$) or, in other words, the nasal retina became shallower as the retina became thinner. Similar correlations in each quadrant are exhibited when examining inner retinal thickness (Fig. 4.11b) and outer retinal thickness (Fig. 4.11c). This result may be consistent with greater eye growth, and hence retinal stretching, on the nasal side of the fovea.

Retinal thickness was also compared to retinal contour at 30 degrees eccentricity to see if the similar correlations exist in the peripheral retina. At 30 degrees, the inverse correlation between full, inner, and outer retinal thickness and depth continue in the superior, inferior, and temporal retinal quadrants (Fig. 4.12). The effect was significant for the superior and inferior retina when examining the full thickness ($p=0.017$; $r^2=0.123$ and $p=0.012$; $r^2=0.192$, respectively) and the inner layer ($p=0.021$; $r^2=0.116$ and $p=0.002$; $r^2=0.206$, respectively), and significant for the inferior retinal outer layer ($p=0.021$; $r^2=0.116$). However, there is no longer a correlation exhibited in the nasal retina. Thus the peripheral retinal data support the general association of greater retinal depth, or steeper contour, with thinner retina in myopia.

(a)



(b)



(c)

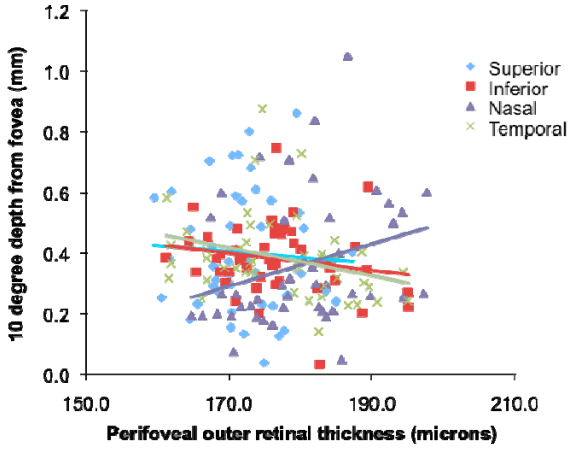
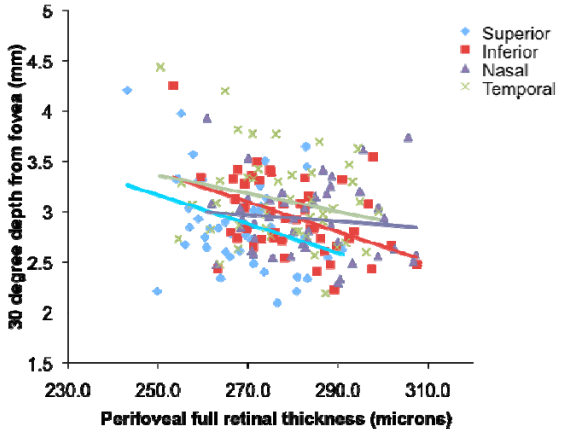
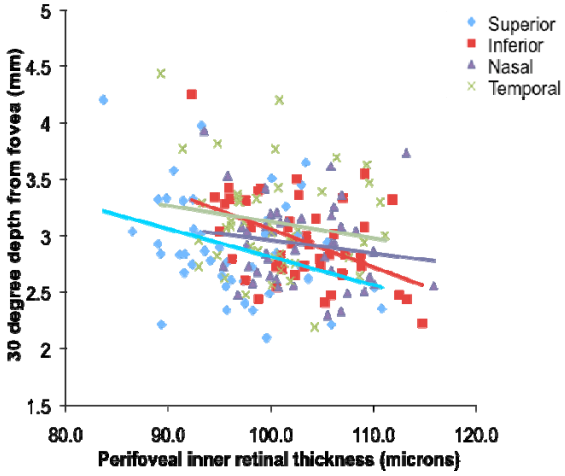


Fig. 4.11. Perifoveal retinal thickness and depth from the fovea at 10 degrees eccentricity by retinal quadrant. Full (a), inner (b), and outer (b) retinal thickness plotted separately.

(a)



(b)



(c)

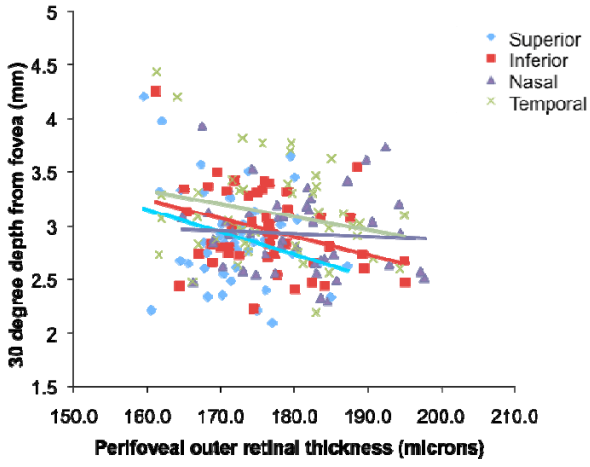


Fig. 4.12. Perifoveal retinal thickness and depth from the fovea at 30 degrees eccentricity by retinal quadrant. Full (a), inner (b), and outer (b) retinal thickness plotted separately.

5. Discussion

5.1 Retinal thickness

The variation of retinal thickness with axial length was examined for the foveal, parafoveal, and perifoveal regions, by retinal quadrant and with respect to inner and outer retinal layers. In the parafoveal region, there was no significant change in full, inner, or outer retinal thickness in any retinal quadrant with axial length. This is in agreement with previous OCT studies of macular thickness change with myopia by Lam et al. (2007) and Song et al. (2010). Other studies, however, have reported thinning in the parafoveal region with myopia (Lim et al. (2005); Wu et al. (2008); Harb et al. (2012)). Differences among studies may be due to differences in the numbers of subjects, the refractive error distribution of the subjects, and differences in OCT devices and analysis software.

In the perifoveal region, subjects with longer axial lengths exhibit retinal thinning in all quadrants. This is in good agreement with previous OCT studies of macular thickness changes with myopia (Lam et al. (2007); Luo et al. (2006); Wu et al. (2008)). The inner retinal layers showed significant thinning in the superior quadrant, while the outer retinal layers showed significant thinning in all four quadrants with axial length.

The central fovea exhibited an increase in full retinal thickness with increasing axial length. This is also consistent with previous OCT studies that have demonstrated foveal thickening with increasing myopia (Lim et al. (2005); Lam et al. (2007); Luo et al. (2006); Harb et al. (2012)). In the central 1 mm region, the inner retinal thickness was shown to increase with axial length, while the outer retinal thickness showed no significant change with axial length. This implies that the increase in foveal thickness in myopic eyes is mainly due to an increase in the inner retinal layers in the central 1 mm

region. Interpretation of this finding must be done with caution, as the OCT software did measure inner retinal thickness at the foveal pit center (Fig. 2.1), as evidenced by the separation of the middle segmentation line from the line demarcating the ILM at the very center of the foveal pit, despite the fact that these inner retinal layers are anatomically absent at the foveal pit center. The OCT software consistently measured inner retinal layer thickness to be about 40-50 microns over the central 1mm region.

5.2 Acuity and retinal thickness

The current study examined the relationship between retinal thickness and acuity in corresponding perifoveal retinal regions. Retinal acuity was demonstrated to decrease with increasing axial length and with increasing myopia in all four perifoveal quadrants. The acuity loss in myopes may be attributed to reduced sampling due to greater cone spacing as a result of retinal stretching (Chui et al., 2008 and Coletta and Watson, 2006), in that measured acuity and acuities predicted from cone spacing fell off with increasing myopia at very similar slopes. Coletta and Watson (2006) measured retinal acuity in healthy subjects at the fovea, 4 deg, and 10 deg temporally using interferometry. The rate of reduction in foveal acuity with myopia measured in the current study is in very close agreement with that measured by Coletta and Watson (2006), as shown in the upper panel of Fig. 5.1, both falling off with a slope of 4.57. Acuity was better in the Coletta and Watson study, and that may be due to the smaller grating patch used in that study (1 deg diameter) compared to the 2 deg diameter fringe patch used in the current study. Naïve subjects may be more accurate at fixating the center of the patch when it is smaller in diameter, and hence may achieve better acuity. Peripheral retinal acuity was measured at

7 deg eccentricity in the current study, and the rate of acuity loss with myopia exhibited in this study in the temporal retina (y=1.5286x+58.936) is comparable to that measured by Coletta and Watson at 4 deg (y=1.344x+78.932).

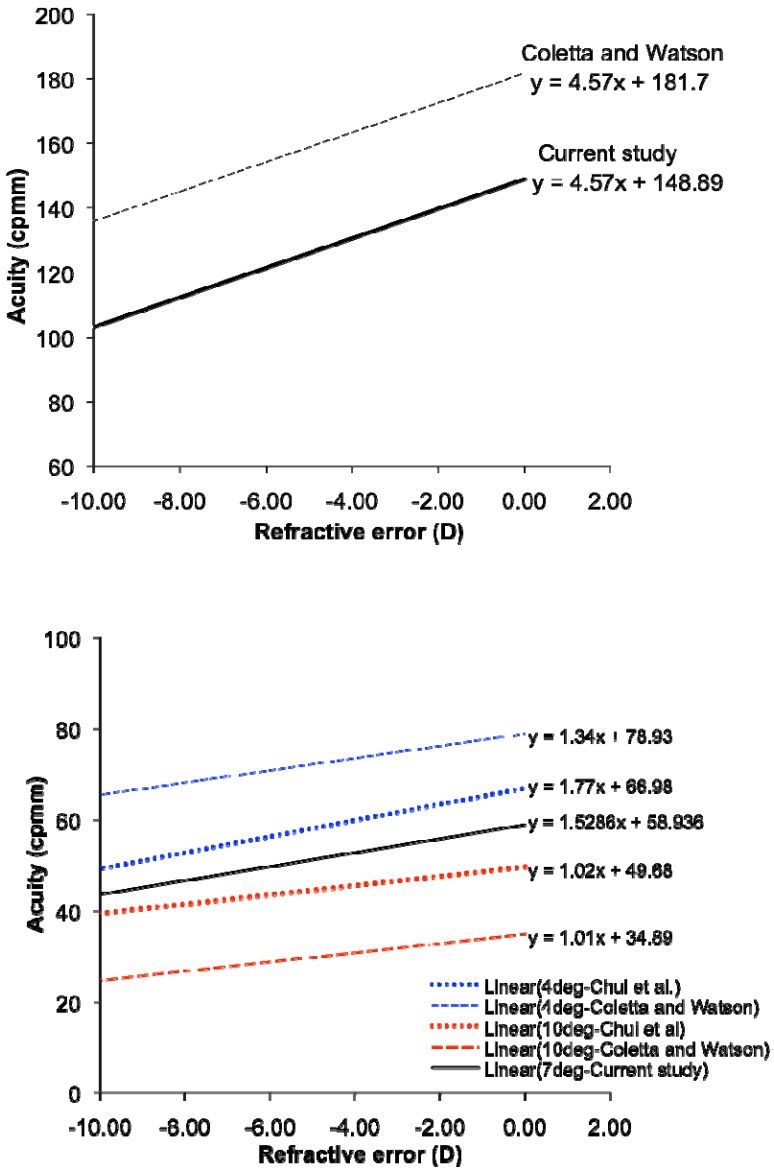


Fig. 5.1 Regression lines of retinal acuity in two psychophysical studies (current study and Coletta and Watson, 2006) and acuity predicted from cone density in retinal images (Chui et al., 2008), as a function of refractive error.

Chui et al. (2006) measured the fall-off in cone density with retinal eccentricity in myopes in four retinal meridians using adaptive optics imaging. They converted their cone density data to acuity in cyc/mm assuming that the Nyquist frequency of the cone mosaic sets the limit for the acuity task. Peripheral acuity predicted from cone density falls off with myopia at similar rates to the measured acuity data in both the 2006 study and the current study (lower panel of Fig. 5.1). Since the rates of fall-off with increasing myopia are similar for the measured acuity and the acuity predicted from cone density, similar amounts of retinal stretching could underlie the results in all three studies.

The 7 deg acuity in the current study is slightly above the cone data at 10 deg but below the cone data at 4 deg. Thus, acuity at 7 deg might match the cone density at about that eccentricity, which would be consistent with a recent finding in other subjects (Coletta et al., ARVO 2013). However, there was not an exact match between the cone density and acuity measures. The cone density predicts higher acuity at 10 deg than the measured acuity at 10 deg in the 2006 study. Peripheral acuity, at least, is considered to be limited by a neural stage after the cones, most likely the midget ganglion cells, which are fewer in number than the peripheral cones beyond about 8-10 deg (Williams and Coletta, 1987; Thibos et al., 1987). Rossi and Roorda (2010) used adaptive optics scanning laser ophthalmoscopy to image the cone mosaic and measured retinal acuity 0-2.5^{o} from the fovea. It was found that visual resolution matched that predicted by cone spacing only at the central fovea (0-0.5^{o}), and peripheral to this, acuity dropped off quicker than cone density predicted, better matching the sampling limit of midget retinal ganglion cells. Results with interference fringes, on the other hand, indicate that high acuity can be achieved even in the parafovea (Williams and Coletta, 1987). The Rossi

and Roorda study used acuity optotypes rather than grating stimuli, so differences in the type of acuity stimulus might explain the discrepancy in acuity limits among these studies. Thus, peripheral retinal acuity measured in the current study could be limited by the ganglion cell mosaic rather than the cone mosaic. Nonetheless retinal stretching that occurs in myopia would be expected to increase the spacing of ganglion cells proportionally with the increase in cone spacing.

Although the current study did not specifically measure properties of the cone photoreceptor layer, retinal thinning may be indicative of retinal stretch and thus decreased cone density. In the current results, there was generally not a strong correlation of retinal acuity with retinal thickness. There was a positive but not significant correlation between retinal acuity and thickness in full and outer retinal layers of the superior perifoveal quadrant. The superior quadrant had the thinnest retina in all layers (Figs. 3.5-3.7) and thus may indicate a region with the most retinal stretching and thus decreased neural density. When ratios of inner/full and outer/full thickness were compared to acuity, the nasal quadrant, and to a lesser degree the temporal quadrant, showed that acuity was higher in eyes that had proportionally greater outer retinal thickness. These results are consistent with outer retinal thickness being associated with higher retinal acuity.

The age of the subjects in this study was restricted to young adults so the current results may not generalize to older eyes. Comparing healthy subjects of different ages, Chui et al. (2012), using AOSLO and SD-OCT imaging, found that older individuals exhibit lower cone packing densities but thicker outer nuclear layer and Henle fiber layers. This increase in outer retinal thickness in older subjects may be attributed to

hypertrophy of Mueller cells, gliosis, and possible retinal remodeling that occurs with age. Thus, variations in cone photoreceptor density may not be reflected in retinal thickness measurements in all age groups.

5.3 Retinal layers and retinal function in myopia

Analysis of inner/full and outer/full retinal thickness ratios allowed for assessment of relative retinal thickness changes of the inner and outer retinal layers. In the parafoveal region, the inner and outer retinal layers showed proportionally constant thinning in all retinal quadrants with increasing axial length. The current study showed that perifoveal retinal thinning in myopia affected both inner and outer retinal layers in all quadrants, but the inner retinal layers of the superior quadrant exhibited proportionally greater thinning with increasing axial length. The inferior, temporal, and nasal quadrants did not show disproportionate thinning of the inner or outer retinal layers in the perifovea. The origin of the greater thinning of the inner retinal layer in the superior retina is unknown, but inner retinal thinning has been noted in other studies. Using time-domain OCT, Wolsley et al. (2008) reported that retinal thinning in myopia was primarily associated with thinning of the middle to inner retinal layers, and reported no thinning of the photoreceptor layer. Similar findings have been reported in tree shrews. Abbott et al. (2011) found that high myopia in tree shrews is correlated with retinal thinning, primarily in the inner plexiform, inner nuclear, and outer plexiform layers, as measured by time-domain OCT and histological assessment.

If mechanical retinal stretching is solely responsible for the overall retinal thinning seen in myopic eyes, then it might be expected that each layer of the retina

would decrease in thickness by an equal proportion. If one retinal layer presents disproportionate thinning compared to others, this could suggest other mechanisms at work besides purely biomechanical stretching, such as functional changes of the retina. Electrodiagnostic studies have elucidated changes in both the outer and inner retinal layers that occur with myopia. Kawabata and Adachi-Usami (1997) conducted multifocal electroretinogram (mfERG) testing on myopes and found reduced amplitudes and delayed latencies associated myopia to be primarily a result of changes in outer retinal function. Chen et al. (2006) compared mfERGs of stable and progressing myopes, specifically looking at the oscillatory potentials, a component thought to arise from the inner retina at the level of the amacrine cells and inner plexiform layer. Significant differences were found between stable and progressing myopes; specifically, progressing myopes had significantly shorter implicit times than stable myopes, suggesting alterations of inner retinal function during myopia development. Chen et al. (2006) theorized that dopaminergic or GABAergic mechanisms are affected by myopia development. Wolsley et al. (2008) reported significantly increased latency of the P1 component of the mfERG in myopes. This component is believed to arise from processing in the middle to inner retina and may be associated with retinal thinning of those layers.

5.4 Retinal contours in myopia

Retinal contour was measured reliably out to 30 degrees eccentricity in the inferior, superior, nasal, and temporal retinal meridians. Readings were attained on some subjects out to 40 deg eccentricity even with the natural pupil. Pupil dilation would be needed to explore peripheral eye lengths reliably at such large retinal eccentricities.

Increased myopia was associated with increased retinal steepness in the periphery when the data are plotted on angular eccentricity units; this finding has been well documented in previous studies of eye shape (Verkicharla et al, 2012). However, larger eyes have larger retinal eccentiricites for the same angular eccentricity and when data are plotted on linear dimensions, retinal contours relative to the foveal position are similar among the different refractive groups.

There were notable asymmetries in retinal contour in low myopes and in high myopes, even when contours were plotted in linear eccentricity units. In high myopes, the temporal retina was steeper than in all other refractive groups, and the nasal retina was shallower than in all other refractive groups. This result is in good agreement with other studies of eye shape (Ehsaei et al., 2013; Chen et al., 2010; Logan et al., 2004). In particular, Ehsaei et al. (2013) used the IOLMaster to measure peripheral eye lengths out to 30 degrees eccentricity along the vertical and horizontal meridians. Myopic eyes were found to exhibit a relatively steeper retinal profile compared to emmetropes. Asymmetry was noted in the horizontal meridian, with the temporal retinal contour being steeper than the nasal contour (i.e., shorter peripheral eye lengths on the temporal side).

Studies measuring peripheral refraction to derive eye shape also showed a similar nasal-temporal asymmetry. Chen et al. (2010) measured peripheral refraction to determine eye shape in children and adult eyes. A nasal-temporal asymmetry was found, in which the temporal retina at 40 degrees eccentricity showed a greater hyperopic shift compared to the nasal retina in myopes. Logan et al. (2004) derived retinal contours from peripheral refraction out to 35 degrees along the horizontal meridian in Chinese and white anisomyopes. The more myopic eyes showed significant outward displacement of

retinal contours. Asymmetry was noted in white eyes, in which the temporal retina exhibited greater retinal steepness than the nasal retina. The nasal-temporal asymmetry in myopes has been interpreted as evidence for greater expansion of the nasal side of the eye compared to the temporal side. The position of the optic nerve may play a role in the observed nasal-temporal asymmetry in retinal contour. The optic nerve head may act as an anchor during myopic eye growth, as a force pulling the retina posteriorly on the nasal side.

In the current study, there was also an asymmetry in the vertical meridian in the low myope group. The inferior meridian showed increased retinal steepness compared to the superior meridian. This effect, however, was no longer observed when all myopes were grouped. This effect has not been reported in other studies of peripheral eye shape but this may be due to the grouping of all myopes across a wide refractive error range.

Retinal contour is largely controlled by the location of the scleral shell, with some contribution from choroidal thickness (Rada et al., 2006). With this in mind, asymmetries in retinal contour likely reflect regional changes in scleral growth patterns. Biochemical and histological studies using animal models have shown differential regulation of scleral growth, with the posterior sclera exhibiting greater change than the equatorial region (McBrien et al., 2001; Rada et al., 2000).

Retinal shape near the fovea was correlated with perifoveal retinal thickness in the current study. When retinal thickness was compared to retinal depth coordinates in the region near the OCT measurements, retinal thinning on the nasal side was significantly correlated with shallower retinal depth (Fig. 4.11). This implies that greater expansion of the nasal side of the eye, at least between the optic nerve head and fovea, is associated

with retinal thinning. In addition, perifoveal retinal thickness in myopia was thinnest overall in the superior quadrant, with the greatest thinning effect exhibited by the inner retina in particular (Figs. 4.9-4.10 and 3.5-3.7). The vertical asymmetry of retinal contour noted in low myopes indicates that the superior retinal meridian is shallower than the inferior meridian, implying greater eye expansion on the superior side of the fovea. It is possible that a relatively posterior displacement of the superior retinal contour is also associated with increased retinal stretch as the globe expands.

There was an inverse correlation between retinal thickness and retinal depth at 30 degrees eccentricty in the superior, inferior, and temporal regions. That is, increased retinal depth or steepness in the periphery was associated with retinal thinning. However, the retinal thickness data are taken from the perifovea, not the peripheral retina, so this association may not be indicative of retinal stretching and eye growth patterns. The current study was limited by the fact that retinal thickness measurements were only attainable at the macular region. Macular thickness measurements may not reflect the changes in retinal thickness in the periphery where the greatest changes in retinal contour are observed in myopes. The perifoveal region lies about 6-8 degrees eccentric to the fovea, and the retinal contours generally do not show significant variation between refractive groups until 20 degrees eccentricity and beyond. No studies have been done to date investigating peripheral retinal thickness and eye shape. Future OCT studies correlating retinal thickness and eye shape at corresponding locations in the peripheral retina would be beneficial.

5.5 Summary and Conclusions

This study examined the relationship between retinal thickness and acuity in myopia. The perifoveal region exhibited retinal thinning with myopia, consistent with most previous OCT studies. The superior retina was the thinnest of the retinal quadrants, showing greatest relative thinning of the inner retinal layer. Myopes also demonstrated losses in retinal acuity in both the fovea and perifoveal regions. The rate of fall-off in acuity is consistent with the rate of fall-off in cone density in myopes, indicating that acuity loss in myopia is at least partially attributable to increased cone spacing. Retinal thickness was generally not significantly correlated with acuity, except that acuity in the superior region was positively associated with perifoveal retinal thickness. In the horizontal meridian, thinning of the outer retinal layer was associated with poorer acuity, consistent with the idea that better acuity is associated with proportionally greater outer retinal layer thickness.

Myopic eye growth was characterized by examining changes in regional retinal contours with refractive error. Increasing myopia and axial length were associated with steeper retinal contours out to an angular eccentricity of 30 degrees in the vertical and horizontal meridians. The retinal contours become more similar between refractive groups when plotted against linear eccentricity to control for eye size, but asymmetries in retinal contour remain. Temporal retina was relatively steeper than the nasal retina in high myopes, and the inferior retina was relatively steeper than the superior retina in low myopes. The nasal-temporal asymmetry is consistent with that reported by previous studies of eye shape. These asymmetries suggest that myopes exhibit greater eye growth, or posterior expansion, in the nasal and superior regions. Retinal thickness in the nasal

perifoveal region did exhibit thinning with shallower retinal contour, indicating retinal stretch occurring with ocular expansion. However, this effect was not seen in any other retinal region.

Regional variations exist in myopic eye growth, resulting in local differences in retinal thickness, retinal contour, and acuity. Myopia is associated with retinal thinning, steepening retinal contour, and poorer acuity when examining these measures independently. Acuity loss was associated with retinal thinning in some retinal regions, and shallower retinal contour was associated with retinal thinning in some regions, as well. However, these associations were not consistent throughout the retina. Larger scale studies are needed to further examine the complex interactions between these factors in myopia development.

6. Bibliography

Abbott CJ, Grünert U, Pianta MJ, McBrien NA. (2011) Retinal thinning in tree shrews with induced high myopia: optical coherence tomography and histological assessment. *Vision Res.* Feb 9;51(3):376-85.

Atchison, D., & Charman, W. (2011). Can partial interferometry be used to determine retinal shape? *Optometry and Vision Science , 88* (5), 601-607.

Atchison, D., Jones, C., Schmid, K., Pritchard, N., Pope, J., Strugnell, W., et al. (2004). Eye shape in emmetropia and myopia. *Investigative Ophthalmology and Visual Science , 45* (10), 3380-86.

Atchison, D., Schmid, K., & Pritchard, N. (2006). Neural and optical limits to visual performance in myopia. *Vision Research , 46* (21), 3707-22.

Chen JC, Brown B, Schmid KL. (2006) Evaluation of inner retinal function in myopia using oscillatory potentials of the multifocal electroretinogram. *Vision Res.* 2006 Nov;46(24):4096-103.

Chen X, Sankaridurg P, Donovan L, Lin Z, Li L, Martinez A, Holden B, Ge J. (2010) Characteristics of peripheral refractive errors of myopic and non-myopic Chinese eyes. *Vision Res*. Jan;50(1):31-5.

Choi, S., Garner, L., & Enoch, J. (2003). The relationship between the Stiles-Crawford effect of the first kind (SCE-1) and myopia. *Ophthalmic & Physiological Optics , 23* (5), 465-72.

Chui TY, Yap MK, Chan HH, Thibos LN. (2005) Retinal stretching limits peripheral visual acuity in myopia. *Vision Res*. Mar;45(5):593-605.

Chui, TY, Song, H., & Burns, S. (2008). Individual variations in human cone photoreceptor packing density: variations with refractive error. *Investigative Ophthalmology & Visual Science , 49* (10), 4679-87.

Coletta, N.J. (2011) Retinal thickness in myopia after adjustment for axial length variation. *ARVO E-abstract* #3209.

Coletta N.J., Chui T. Y. and Elsner AE. (2013) A comparison of acuity and cone density in the temporal retina. *ARVO E-abstract* #4064.

Coletta, N., & Watson, T. (2006). Effect of myopia on visual acuity measured with laser interference fringes. *Vision Research , 46* (5), 636-51.

Curtin, B. (1985). *The myopias: basic science and clinical management.* Michigan: Harper & Row.

Deller, J., O'Connor, A., & Sorsby, A. (1947). X-ray measurement of the diameters of the living eye. *Proceedings of the Royal Society of Medicine , 134*, 456-467.

Ehsaei, A., Chisholm, C., Pacey, I., & Mallen, E. (2013). Off-axis partial coherene inerferometry in myopes and emmetropes. *Ophthalmic & Physiological Optics , 33*, 26-34.

Flores-Moreno, I., Lugo, F., Duker, JS, Ruiz-Moreno, JM. (2013). The relationship between axial length and choroidal thickness in eyes with high myopia. *American Journal of Ophthalmology* , 155(2), 314-319.

Harb, E., Hyman, L., Fazzari, M., Gwiazda, J., Marsh-Tootle, W., & Group, C. S. (2012). Factors associated with macular thickness in the COMET myopic cohort. *Optometry and Vision Science , 89* (5), 620-31.

Hendrickson, A. (1992). A morphological comparison of foveal development in man and monkey. *Eye , 6*, 136-44.

Kawabata H, Adachi-Usami E. (1997) Multifocal electroretinogram in myopia. *Invest Ophthalmol Vis Sci.* Dec;38(13):2844-51.

Kitaguchi Y., Bessho K., Yamaguchi T., Nakazawa N., Mihashi T., Fujikado T. In vivo measurements of cone photoreceptor spacing in myopic eyes from images obtained by an adaptive optics fundus camera. *Japanese Journal of Ophthalmology*:2007 vol:51 iss:6 pg:456 -461.

Lam, A. K., Chan, R., & Pang, P. C. (2001). The repeatability and accuracy of axial length and anterior chamber depth measurements from the IOLMaster. *Ophthalmic & Physiological Optics*, 21, 477–483.

Lam, D., Leung, K., Mohamed, S., Chan, W., Palanivelu, M., Cheung, C., et al. (2007). Regional variations in the relationship between macular thickness measurements and myopia. *Investigative Ophthalmology & Visual Science , 48* (1), 376-82.

Lim, M., Hoh, S., Foster, P., Lim, T., Chew, S., Seah, S., et al. (2005). Use of optical coherence tomography to assess variations in macular retinal thickness in myopia. *Investigative Ophthalmology & Visual Science , 46* (3), 974-8.

Logan, N., Gilmartin, B., Wildsoet, C., & Dunne, M. (2004). Posterior retinal contour in adult human anisomyopia. *Investigative Ophthalmology & Visual Science , 45* (7), 2152-62.

Luo, H., Gazzard, G., Fong, A., Aung, T., Hoh, S., Loon, S., et al. (2006). Myopia, axial length, and OCT characteristics of the macula in Singaporean children. *Investigative Ophthalmology & Visual Science , 47* (7), 2773-81.

Mallen, E., & Kashyap, P. (2007). Technical note: Measurement of retinal contour and supine axial length using the Zeiss IOLMaster. *Ophthalmic Physiological Optics , 27*, 404-411.

McBrien, N., Cornell, L., & Gentle, A. (2001). Structural and ultrastructural changes to the sclera in a mammalian model of high myopia. *Investigative Ophthalmology & Visual Science , 42* (10), 2179-87.

Mutti, D., Scholtz, R., Friedman, N., & Zadnik, K. (2000). Peripheral refraction and ocular shape in children. *Investigative Ophthalmology and Visual Science , 41* (5), 1022-30.

Mutti, D., Sinnott, L.T., Mitchell, G.L., Jones-Jordan, L.A., Moeschberger, M.L., Cotter, S.A., Kleinstein, R.N., Manny, R.E., Twelker, J.D., Zadnik, K., CLEERE Study Group (2011). Relative peripheral refractive error and the risk of onset and progression of myopia in children. *Investigative Ophthalmology & Visual Science* , 52(1), 199-205.

Pan, C.-W., Ramamurthy, D., & Saw, S.-M. (2011). Worldwide prevalence and risk factors for myopia. *Opthalmic and Physiological Optics , 32*, 3-16.

Rada, J., Nickla, D., & Troilo, D. (2000). Decreased proteoglycan synthesis associated with form deprivation myopia in mature primate eyes. *Investigative Ophthalmology & Visual Science , 41* (8), 2050-8.

Rada, J., Shelton, S., & Norton, T. (2006). The sclera and myopia. *Experimental Eye Research , 82* (2), 185-200.

Rossi EA, Roorda A. (2010) The relationship between visual resolution and cone spacing in the human fovea. *Nat Neurosci*. Feb;13(2):156-7.

Sahin, A. and Hamrah, P. (2012). Clinically relevant biometry. *Current Opinion in Ophthalmology* , 23(1), 47-53.

Sato, A., Fukui, E., & Ohta, K. (2010). Retinal thickness of myopic eyes determined by spectralis optical coherence tomography. *British Journal of Opthalmology , 94* (12), 1624-28.

Saw, S.-M., Gazzard, G., & Chan Shih-Yen, E. (2005). Myopia and associated pathological complications. *Opthalmic and Physiological Optics , 25*, 381-391.

Schmid, G. (2003). Variability of retinal steepness at the posterior pole in children 7-15 years of age. *Current Eye Research , 27* (1), 61-68.

Sheng, H., Bottjer, C. A., & Bullimore, M. A. (2004). Ocular component measurement using the Zeiss IOLMaster. *Optometry and Vision Science*, 81, 27–34.

Sng, C.C., Lin, X.Y., Gazzard, G., Chang, B., Dirani, M., Lim, L., Selvaraj, P., Ian, K., Drobe, B., Wong, TY, Saw, S.M. (2011) Change in peripheral refraction over time in Singapore Chinese children. *Investigative Ophthalmology & Visual Science*, 52(11), 7880-7.

Song, H., Kim, Y., Lee, S., & Moon, Y. (2007). Relations between age, weight, refractive error and eye shape by computerized tomography in children. *Korean Journal of Ophthalmology , 21* (3), 163-168.

Song, W., Lee, S., Lee, E., Kim, C., & Kim, S. (2010). Macular thickness variations with sex, age, and axial length in healthy subjects: A spectral domain-optical coherence tomography study. *Investigateive Ophthalmology & Visual Science , 51* (8), 3913-18.

Strang, N., Winn, B., & Bradley, A. (1998). The role of neural and optical factors in limiting visual resolution in myopia. *Vision Research , 38* (11), 1713-21.

Thibos LN, Walsh DJ, Cheney FE. (1987) Vision beyond the resolution limit: aliasing in the periphery. Vision Res. ;27(12):2193-7.

Vera-Diaz, F., McGraw, P., Strang, N., & Whitaker, D. (2005). A psychophysical investigation of ocular expansion in human eyes. *Investigative Ophthalmology and Visual Science , 46* (2), 658-63.

Verkicharla PK, Mathur A, Mallen EA, Pope JM, Atchison DA. (2012) Eye shape and retinal shape, and their relation to peripheral refraction. *Ophthalmic Physiol Opt.* May;32(3):184-99.

Wallman, J., & Winawer, J. (2004). Homeostasis of eye growth and the question of myopia. *Neuron , 43*, 447-68.

Wertheim T. (1980) Peripheral visual acuity: Th. Wertheim. *Am J Optom Physiol Opt.* Dec;57(12):915-24.

Williams, D., & Coletta, N. (1987). Cone spacing and the visual resolution limit. *Journal of the Optical Society of America , 4* (8), 1514-23.

Wolsley CJ, Saunders KJ, Silvestri G, Anderson, RS. (2008). Investigation of changes in the myopic retina using multifocal electroretinograms, optical coherence tomography and peripheral resolution acuity. *Vision Research, 48*(14), 1554-1561.

Wu, P., Chen, Y., Chen, C., Shin, S., Yang, H., & Kuo, H. (2008). Assessment of macular retinal thikness and volume in normal eyes and highly myopic eyes with third-generation optical coherence tomography. *Eye (Lond) , 22* (4), 551-555.

Xie, R., Zhou, X., Lu, F., Chen, M., Xue, A., Chen, S., et al. (2009). Correlation between myopia and major biometric paramters of the eye: A retrospective clinical study. *Optometry and Vision Science , 86* (5), 530-508.

7. Appendix

7.1 Consent form

THE NEW ENGLAND COLLEGE OF OPTOMETRY
424 Beacon Street
Boston, MA 02115
Tel: 617.266.2030
Fax: 617.424.9202

STATEMENT OF INFORMED CONSENT

Retinal Thickness, Eye Shape and Visual Acuity: Effects of Refractive Error

Overview

You are being asked to volunteer to participate in a research project to study the effect of refractive error (nearsightedness or farsightedness) on visual acuity, and its relationship to retinal thickness and eye shape. The testing will require two visits that will be scheduled at your convenience. The testing will take place at New England College of Optometry and is expected to take approximately 2 hours per visit. The study will involve up to 40 subjects.

We will measure your refractive prescription, corneal power (curvature of the front of the eye), retinal thickness and eye measurements such as eye length and eye shape. We will also measure your visual acuity (test for your ability to see fine patterns and letters), using charts and an optical system. All of these tests are non-invasive. All but one of these tests are available to you outside of this study. The remaining test, laser interferometry, involves a custom optical system that has been safely used in human studies with no adverse effects.

Description of Tests & Procedures

The same tests and procedures will be performed on all subjects. After obtaining your eye history and an initial refraction and acuity assessment of your left eye, all subsequent testing will be performed on your left eye.

Visual acuity (determine your ability to see small letters): You will be asked to read letters on a printed chart. We will test the left eye and this eye will be used for all subsequent testing. To qualify for participation in the study, you must have 20/30 or better corrected acuity in the left eye.

Autorefraction and Aberrometry (refractive prescription and optical quality of the eye): The COAS autorefractor will measure the refractive error and the optical quality (aberrations) of your eye by recording images of light passing through the eye. You will be seated at a chinrest and forehead restraint in front of the device and asked to fixate a ring target. Mutliple pictures will be taken of your eye, in various positions of gaze, from which the refraction of the entire eye will be determined.

Corneal Power (curvature of the front of the eye) and Eye Length and Eye Shape Measurement:
You will be seated at a chin rest and head restraint of the IOL Master instrument, and a live image of your eye will be viewed while you fixate a light. Several pictures will be taken of your eye, from which the instrument will determine the surface curvature of your cornea. Next you will fixate a light or a point on a card so that your eye length can be measured in several positions of eye gaze; 20 measurements will be taken. From these measurements, your eye length and shape will be determined.

Retinal Thickness Imaging: You will be seated in front of the Optovue RTVue instrument at a chinrest and forehead restraint and asked to fixate a target. This optical coherence tomography (OCT) instrument will measure the thickness of your retina by recording images of light passing through the eye. Several pictures will be taken of your eye, from which the retinal thickness will be determined.

Visual acuity for grating patterns (laser interferometry - determines your ability to see fine stripes):
For this test, you will be shown a series of grating (striped) patterns, some of which you will be able to detect and others which will not be visible to you. On each trial, the striped pattern will be presented in one of two stripe orientations (vertical or horizontal), and you will be asked to indicate the direction of stripes. This is a "forced-choice" procedure, meaning that you must respond even if you did not detect the pattern. You will control presentation of the stripes with a joystick. This test involves repeated presentations and may become tedious. You will be allowed to take breaks as needed.

Possible Discomforts or Risks

The procedures have been safely used on human subjects and present no foreseeable discomforts or risks. Some procedures may present a bright light to your eye, but this light is no brighter than what you would experience during a routine eye exam. However these procedures may involve risks that are unforeseeable.

The tedious nature of acuity experiments may present some minor discomfort to you. To avoid fatigue during these measurements, the procedures will be self-paced and you will be allowed to take breaks whenever possible during testing. Chair heights as well as chin and head rests are adjustable.

This study presents minimal risks. In the unlikely event of injury resulting from your participation in this study, contact Dr. Coletta at 617-587-5681. If she is not available, or in an emergency, call the New England Eye Institute at 617-262-2020, or go to the emergency room of a hospital. You and/or your healthcare insurance are responsible for payment for this treatment.

Benefits

Your participation in this study will contribute to our understanding of the relationship of refractive error to eye shape, retinal thickness and visual performance. There are no direct benefits to you from participating in this study. You will be given $40 within two weeks of completion of the study, in appreciation for your effort and to help defray transportation costs.

Confidentiality

Your medical records will be kept as confidential as possible within the limitations of state and federal law.

If you decide to be a subject in this study, both demographic and technical information about you will be collected. Demographic information will include, but will not be limited to such things as, your name, date of birth, address, gender, ethnicity, etc. Technical information will include elements of your personal health history and results of all the tests and measurements related to the study. This information is collected in order to determine whether you are eligible to be a subject in the study; that is, to meet the inclusion/exclusion criteria and, if so, to allow the study investigators to gather the data from you that is necessary to support the study's purpose. The results from all of the subjects in the study can then be analyzed to develop the study's conclusion.

All study-related information will remain confidential with the investigators and administrative staff at NECO. However, any regulatory authority or the Institutional Review Board may inspect the investigators' records pertaining to you as a subject. But they too should maintain confidentiality.

The results of the study may be used in health care education or in scientific publications. Neither your name nor any information that specifically could identify you will be used in any such presentation or publication.

Personal Health Information

Your personal health information (PHI), as related to this study, is described in the "Confidentiality" section above. If you sign this informed consent form, it grants permission to use your PHI as specifically discussed. This permission does not have an expiration date, but you can cancel it at any time by writing to the principal investigator(s) at the address below.

If you cancel your permission to use your PHI after you have started the study but before your study participation would normally be concluded, you will not be allowed to continue

in the study and the investigators will stop collecting data. However, they retain the right to use the information they have already collected to evaluate the study's results.

Privacy Practices and Your Rights

Health care providers are required by law to keep private any health information that identifies people. Federal Privacy Regulations require that you authorize the release of any health information that may reveal your identity. The persons and entities that you are authorizing to use or inspect all of the health information generated or collected about you during this study includes the study doctor(s), the study staff, the Institution, any study Sponsor (or the authorized agents of the sponsor), the Food and Drug Administration (FDA), the Department of Health and Human Services (DHHS) agencies, and the Institutional Review Board. Because of the need to release information to these parties absolute confidentiality cannot be guaranteed. Once your personal health information is released it may be redisclosed, at which point your health information may no longer be protected by federal privacy regulations.

You may ask the study investigator to see a copy of your PHI related to the study. You may also request the study investigator to correct any information that you feel is incorrect. However, you may have to wait until the end of the study to see your records so that the study can be organized and conducted scientifically.

You must be given notice of your investigator's privacy policies. The Confidentiality, Personal Health Information, and Privacy Practices and Your Rights sections of this form fulfill this requirement.

Unless you authorize the use and disclosure of your personal health information, you cannot participate in this research study. If you refuse to give your authorization, your medical care will not be affected.

Voluntary Participation/Withdrawal from the Study

Participation in this study is voluntary and you may withdraw at any time. Refusal to participate or withdrawal from the study will not involve any penalty or loss of benefits to which you are otherwise entitled. If you are a student at NECO, your participation or withdrawal will not affect your academic standing. If you are a NECO staff or faculty member, your participation or withdrawal will not affect your position at the College. We will disclose to you in a timely manner any significant new findings that may influence your willingness to participate in the study.

The investigators or the Institutional Review Board may terminate your participation in the study (with or without your consent) if it is believed to be in your best interest.

Questions

Any questions you may have about this study or about your rights as a study participant may be directed to the investigator, Dr. Nancy J. Coletta (617-587-5681). You may also

contact Dr. Paul White (617-266-2030 ext 5251), Chairman of the Institutional Review Board of the New England College of Optometry, 424 Beacon Street, Boston MA 02115.

Voluntary Consent

I have read this consent form and I understand it. Any questions concerning this study have been answered to my satisfaction and I have been offered a copy of this consent form. By signing this form, I voluntarily agree to participate in this study.

I understand the potential risks and benefits involved in this study and that I may withdraw at any time without penalty. I understand that I must notify the study investigator immediately if I notice any medical problems that may be related to my participation in the study. I also understand that my participation in the study may be terminated at any time if the investigators or the Institutional Review Board feel that it in my best interest or if I fail to keep the required study appointment(s) or follow the study instructions.

I understand that the study records may be inspected by the Institutional Review Board.

_____

Subject's Name (PRINT)

_____ _____

Signature of Subject Date

_____ _____

Signature of Witness Date

_____ _____

Signature of Investigator (or Designee) Date

7.2 Recruitment message

Retinal Thickness, Eye Shape and Visual Acuity: Effects of Refractive Error

To: NECO Students, Faculty & Staff
From: Dr. Nancy J. Coletta
Re: Volunteers for Research Study

We are recruiting up to 40 volunteers to participate in a study of how visual acuity, retinal thickness and eye shape are related in myopic and emmetropic individuals.

We plan to measure your refractive error, visual acuity, corneal power, eye length and retinal thickness, all of which are non-invasive tests that will be performed using conventional clinical devices. We will also measure your visual acuity with fine striped patterns that are displayed in a non-invasive custom-built optical system.

We are currently enrolling adults, aged 18 and older, who are in good general health and have good vision, with or without correction. To be included in the study, you must have best-corrected visual acuity of 20/30 or better in the left eye. You may wear spectacles or contact lenses. Refractions can fall within the range from hyperopia (up to +2.00D) to high myopia (up to -12.00 D), with up to 1.75 D of astigmatism.

People with the following characteristics are NOT eligible for the study: history of ocular pathology, eye injury or surgery, present ocular medications, cataract or other media opacity, fixational instability (e.g., nystagmus) or restricted movement of either eye. In addition, we plan to exclude users of ortho-K or Corneal Refractive Therapy contact lenses.

We estimate that all measurements can be completed in two visits to the laboratory. The total duration of the testing will be approximately 4 hours, divided into two visits of about 2 hours each. In appreciation of your time and effort, you will be given $40 within three weeks of the completion of your 2 visit. If you have questions or wish to participate, please contact Dr. Nancy Coletta by e-mail (colettan@neco.edu) or phone (617-587-5681).

Please provide the following information:1) name and age, 2) phone number and/or e-mail address, 3) best days and times for your appointment and 4) approximate refraction.

The above information is needed to help organize the subject groups and will be maintained in confidence. The testing will be done in Dr. Coletta's lab at 424 Beacon St. We will schedule the appointments at your convenience.

Thanks for your help,
Nancy J. Coletta, O.D., Ph.D., FAAO
Stephanie Shao, OD/MS 2013

7.3 Questionnaire

Retinal Thickness, Eye Shape and Visual Acuity: Effects of Refractive Error

Name _____ Date of Birth _____

Gender ____ M ____ F

Eye History:

1. When was your most recent eye exam? _____

2. Do you have any current or past eye pathology? ____ yes ____ no

   If yes, please describe:
   _____

   _____

3. Have you had any eye injuries? ____ yes ____ no

   If yes, please describe:
   _____

   _____

4. Have you had eye surgery including refractive eye surgery? ____ yes ____ no

If you wear contact lenses, please answer questions #5 - 10:

Contact Lens Wear:

5. What type of lenses do you wear?

   ____ soft hydrogel ____ silicone hydrogel ____ rigid gas permeable

   ____ daily wear ____ extended wear ____Corneal Refractive Therapy*

   ____ single vision ____ multifocal

***If you wear CRT lenses or ortho-K lenses, you may not participate in the study.**

6. How long have you worn the type of lenses you are currently wearing? ____ years

7. Did you wear a different type of lenses prior to your current lenses?
____ yes ____ no

If yes, what type of lenses did you previously wear? _____
For how long? ____ years

8. How many days per week do you typically wear your lenses? ____ days

9. How many hours per day do you typically wear your lenses? ____ hours

10. Have you had any problems with your lenses? ____ yes ____ no

If yes, please describe:
_____